Chapter 19. Orbiting the Spinning Black Hole

- *As my spaceship approaches the spinning black hole, how do I insert it into an initial circular orbit?*
- *Which of the four Types of circular orbits at a given r do I choose?*
- *How can I transfer from one circular orbit to a closer one?*
- *Can I put a probe into a circular orbit inside the Cauchy horizon?*
- *Can I harness the black hole spin to "throw" stones (or photons) out to a great distance?*
- *At what r-value do tides in a circular orbit become lethal?*

CHAPTER 19 Orbiting the Spinning Black Hole

Edmund Bertschinger & Edwin F. Taylor *

Einstein was not only skeptical, he was actively hostile, to the idea of black holes. He thought the black hole solution was a blemish to be removed from the theory by a better mathematical formulation, not a consequence to be tested by observation. He never expressed the slightest enthusiasm for black holes, either as a concept or a physical possibility.

—Freeman Dyson

19.1 ■ EXPLORE THE SPINNING BLACK HOLE

The sequence of orbits in our exploration plan

Observe the black hole from circular orbits.

Chapter 18 described circular orbits of a free stone around a spinning black hole. The present chapter shows how the captain of an approaching spaceship can insert her ship into an initial circular orbit at arbitrarily-chosen $r = 20M$, then transfer to circular orbits of progressively smaller r-value to provide closer looks at the black hole.

The exploration program for the spinning black hole is similar to that for the non-spinning black hole (Chapter 9) but in some ways strikingly different. In particular, the spinning black hole may be monitored from unstable circular orbits *inside* the Cauchy horizon (Step 3 in the following exploration program).

Exploration program

EXPLORATION PROGRAM FOR THE SPINNING BLACK HOLE [$a/M = (3/4)^{1/2}$]

Step 1. Insert the approaching spaceship into an initial stable circular orbit at $r = 20M$.

Step 2. Transfer an observation probe from this initial circular orbit to the innermost stable circular orbit (ISCO) at $r_{\rm ISCO} = 2.5373M$.

Step 3. Transfer the probe from $r_{\rm ISCO}$ into either of two unstable circular orbits *inside the Cauchy horizon.*

Step 4. Tip the probe off the unstable circular orbit so that it spirals into the singularity.

*Draft of Second Edition of *Exploring Black Holes: Introduction to General Relativity*

Box 1. Useful Relations for the Spinning Black Hole

This box repeats Box 1 in Section 17.8.

Static limit from Section 17.3:

$$r_\mathrm{S} = 2M \tag{1}$$

Reduced circumference from Section 17.2:

$$R^2 \equiv r^2 + a^2 + \frac{2Ma^2}{r} \tag{2}$$

Horizon function from Section 17.3:

$$H^2 \equiv \frac{1}{r^2}\left(r^2 - 2Mr + a^2\right) \tag{3}$$

$$= \frac{1}{r^2}\left(r - r_\mathrm{EH}\right)\left(r - r_\mathrm{CH}\right) \tag{4}$$

where r_EH and r_CH are r-values of the event and Cauchy horizons, respectively, from Section 17.3.

$$\frac{r_\mathrm{EH}}{M} \equiv 1 + \left(1 - \frac{a^2}{M^2}\right)^{1/2} \quad \text{(event horizon)} \tag{5}$$

$$\frac{r_\mathrm{CH}}{M} \equiv 1 - \left(1 - \frac{a^2}{M^2}\right)^{1/2} \quad \text{(Cauchy horizon)} \tag{6}$$

Ring omega from Section 17.3:

$$\omega \equiv \frac{2Ma}{rR^2} \tag{7}$$

An equivalence from Section 17.3:

$$1 - \frac{2M}{r} + R^2\omega^2 = \left(\frac{rH}{R}\right)^2 \tag{8}$$

Definition of α from Section 17.7:

$$\alpha \equiv \arcsin\left[\left(\frac{2M}{r}\right)^{1/2}\frac{a}{rH}\right] \quad (0 \leq \alpha \leq \pi/2) \tag{9}$$

Definition of β from Section 17.8:

$$\beta \equiv \left(\frac{2M}{r}\right)^{1/2}\left(\frac{r^2 + a^2}{R^2}\right)^{1/2} \tag{10}$$

Compare with the non-spinning black hole.

This chapter does not contain queries that ask you to “Compare these results with those for a non-spinning black hole.” Nevertheless, we recommend that you do so automatically: Run your finger down the text of Chapter 9 as you read Chapter 19. The similarities are as fascinating as the differences!

Box 1 reminds us of useful relations for the spinning black hole, taken from earlier chapters. Box 2 clarifies what it means to plot the orbits of a stone.

REVIEW FROM CHAPTER 18: KINDS OF MOTION

Classify the motion of a stone by how its Doran global coordinates change during that motion. Section 18.5 defined prograde/retrograde motion and also forward/backward motion as follows:

Kinds of motion

- **Prograde motion** has $d\Phi/d\tau > 0$.
- **Retrograde motion** has $d\Phi/d\tau < 0$.
- **Forward motion** has $dT/d\tau > 0$.
- **Backward motion** has $dT/d\tau < 0$.

Recall that the raindrop (released from rest far from the black hole) falls with $d\Phi/d\tau = 0$ (Section 17.4). Raindrop motion provides the dividing line between prograde and retrograde motion.

Wristwatch time τ runs forward along the worldline of a stone. In backward motion ($dT/d\tau < 0$), map T runs backward along the stone’s worldline—a reminder that map coordinate T is *not* measured time.

Sections 18.4 and 18.5 described four Types of circular orbits:

REVIEW: FOUR TYPES OF CIRCULAR ORBITS

Types of circular orbits

- **Type 1 Circular:** $E/m > 0$, $L/m > 0$, forward, prograde, with $E/m = V_{\mathrm{L}}^{+}$
- **Type 2 Circular:** $E/m < 0$, $L/m < 0$, backward, prograde, with $E/m = V_{\mathrm{L}}^{-}$
- **Type 3 Circular:** $E/m < 0$, $L/m > 0$, backward, retrograde, with $E/m = V_{\mathrm{L}}^{+}$
- **Type 4 Circular:** $E/m > 0$, $L/m < 0$, forward, retrograde, with $E/m = V_{\mathrm{L}}^{-}$

Note: In Type 1 and 2 orbits, the signs of E/m and L/m apply outside the event horizon. Inside the Cauchy horizon the signs may be different. (Table 3, Section 18.5).

In addition to circular orbits, the present chapter studies a series of transfer orbits that take us from one circular orbit to another.

Comment 1. Follow the Figures
This chapter continues, even increases, the heavy use of algebra, but it has a simple central theme: how to insert a spaceship into an outer circular orbit, then how to transfer from this outer circular orbit to inner circular orbits. Pay attention to the figures, which illustrate and summarize these transitions.

19.2 ■ INSERT APPROACHING SPACESHIP INTO AN INITIAL CIRCULAR ORBIT

Approach from far away and enter an initial circular orbit.

Insert incoming spaceship into initial circular orbit.

A spaceship approaches the spinning black hole from a great distance. The captain chooses $r = 20M$ for her initial circular orbit, near enough to the spinning black hole to begin observations. How does she manage this insertion? Analyze the following method: While still far from the black hole, the captain uses speed- and direction-changing rocket thrusts to put the spaceship into an unpowered orbit whose minimum r-value matches that of the desired initial circular orbit (Figure 1). At that minimum, when the spaceship moves tangentially for an instant, the captain fires a tangential rocket to slow down the spaceship to the speed in a stable circular orbit at that r-value.

Comment 2. Both unpowered spaceship and unpowered probe = stone
In the present chapter, our spaceship or probe sometimes blasts its rockets, sometimes remains unpowered. The unpowered spaceship or probe moves as a free stone moves. It is important not to confuse powered and unpowered motions of "spaceship" or "probe."

Insertion orbit

What values of map E and L lead a distant incoming unpowered spaceship later to move tangentially for an instant at the chosen $r = 20M$ (Figure 1)? To find out, manipulate equations (15) and (16) in Section 18.2 and introduce the condition $dr/d\tau = 0$ (tangential motion), so that $E = V_{\mathrm{L}}^{\pm}(r)$. The result is:

Box 2. How do we plot orbits of a stone?

This chapter asks and answers two questions about a stone's orbit: **Question 1:** How do we calculate the orbit of a stone? **Question 2:** How do we plot that orbit? Question 2 is a central subject of this chapter.

What is the precise definition of the stone's orbit? Technically **An orbit is a parameterized worldline expressed in global coordinates**. Huh, what does that mean? Here's an example: Go for a walk, during which you glance occasionally at your wristwatch. Later you announce, "When I arrived at the corner of Main and Pleasant Streets, my wristwatch read seven." Wristwatch time is—literally!—the *parameter* by which you report on your walk. Of course, the wristwatch time between two locations depends on the path you choose between them. If you go by way of Lester Street (for example), your wristwatch will record a longer time of, say, ten minutes.

Every orbit plotted in this book is a parameterized worldline expressed in global coordinates. In Doran coordinates, for example, three functions $T(\tau)$, $r(\tau)$, and $\Phi(\tau)$ give a full description of the stone's orbit, parameterized by its wristwatch time τ. On our two-dimensional page we plot the orbit on a two-dimensional slice, typically the $[r, \Phi]$ slice.

Restate the two questions that began this box:
Question 1: How do we obtain these orbit functions?
Question 2: How do we plot these orbit functions?
Answer Question 2 first.

Question 2: For reasons discussed in Section 19.5, we translate r and Φ into Cartesian-like global coordinates $X \equiv (r^2+a^2)^{1/2}\cos\Phi$ and $Y \equiv (r^2+a^2)^{1/2}\sin\Phi$—equations (40) and (41). In these global coordinates the black hole singularity $r = 0$ is a ring with $(X^2 + Y^2)^{1/2} = a$. The X and Y coordinates of an orbit are plotted as if they were Cartesian (Figure 10). (Indeed, behind the scenes we plot every orbit in this book using similar Cartesian-like coordinates, including those plotted by the software GRorbits.)

Back to Question 1, how to obtain functions $r(\tau)$ and $\Phi(\tau)$, is easy to answer in principle but more difficult in practice. In principle, we simply integrate equations of motion for $dr/d\tau$ and $d\Phi/d\tau$—equations (4) and (15) in Section 18.2. In practice, the $\pm$ signs in these equations make them difficult to solve. Instead, our plotting programs—including GRorbits—use different equations of motion defined for $\tau(T), r(T), \Phi(T)$, with global T-coordinate as the parameter (Section 20.1). These equations do not contain $\pm$ signs and are valid provided $d\tau/dT \neq 0$. *Full disclosure:* We do not display these equations, which are based on so-called "Hamiltonian methods."

Objection 1. *Fraud! You just admitted that neither the calculation of orbits nor their plots in this book use the equations of motion you give us. Stop lying to us.*

You're right—and wrong. A wise manager lays out the general strategy to reach a goal, shows an in-principle path to that goal, then delegates to others completion of the project. Shall we take a side trip into "Hamiltonian methods" (whatever that means) to calculate orbits from equations of motion that do not have plus-or-minus signs? We choose not to. Instead we plunge ahead with our story of diving into the spinning black hole.

$$\frac{E}{m} = \omega\frac{L}{m} \pm \frac{rH}{R}\left(1 + \frac{L^2}{m^2R^2}\right)^{1/2} \qquad \text{(tangential)} \qquad (11)$$

Here the $\pm$ on the right side is the same as the superscript on $V_{\mathrm{L}}^{\pm}(r)$. Write (11) as a quadratic equation in L/m:

$$\left[\omega^2 - \left(\frac{rH}{R^2}\right)^2\right]\left(\frac{L}{m}\right)^2 - 2\omega\frac{E}{m}\left(\frac{L}{m}\right) + \left[\left(\frac{E}{m}\right)^2 - \left(\frac{rH}{R}\right)^2\right] = 0 \qquad (12)$$

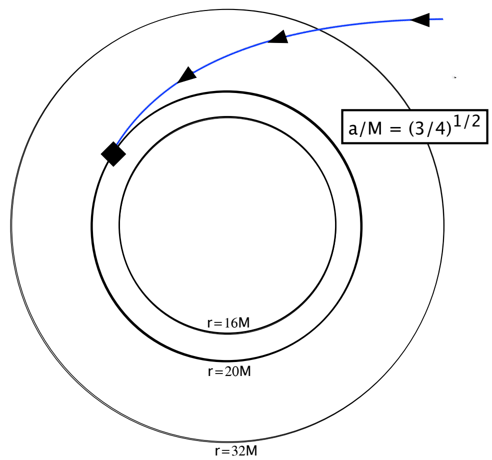

FIGURE 1 An insertion orbit with instantaneous tangential motion at $r = 20M$. At that instant the spaceship fires a tangential rocket burst that reduces the local ring velocity to that for a Type 1 circular orbit there (Figure 2).

This quadratic equation is in the standard form:

$$A\left(\frac{L}{m}\right)^2 - 2B\left(\frac{L}{m}\right) + C = 0 \tag{13}$$

with the standard solution:

$$\frac{L}{m} = \frac{B \pm (B^2 - AC)^{1/2}}{A} \tag{14}$$

Use (8) to simplify coefficient A:

$$A \equiv \omega^2 - \left(\frac{rH}{R^2}\right)^2 = -\frac{1}{R^2}\left(1 - \frac{2M}{r}\right) \tag{15}$$

Show that:

$$B^2 - AC = \left(\frac{rH}{R^2}\right)^2 \left[\left(\frac{E}{m}\right)^2 - \left(1 - \frac{2M}{r}\right)\right] \tag{16}$$

With these substitutions, (14) yields the solution:

$$\boxed{\frac{L}{m} = \frac{-\omega R^2\left(\dfrac{E}{m}\right) \pm rH\left[\left(\dfrac{E}{m}\right)^2 - \left(1 - \dfrac{2M}{r}\right)\right]^{1/2}}{1 - \dfrac{2M}{r}} \qquad \text{(tangential)} \qquad (17)}$$

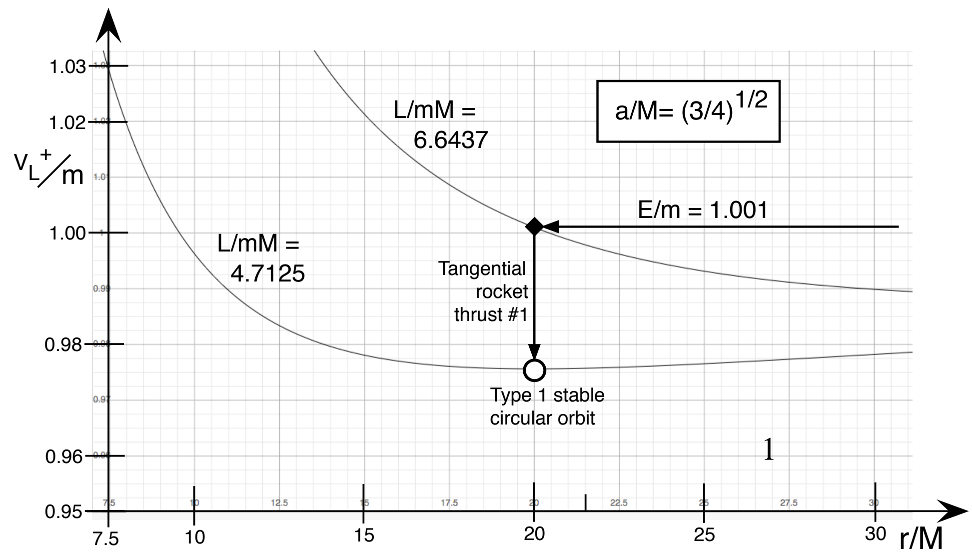

FIGURE 2 At the instant when the incoming spaceship moves tangentially at the turning point $r = 20M$ (Figure 1), it fires tangential rocket thrust #1 to change its map energy and map angular momentum to those for a Type 1 stable circular orbit at that r.

You choose the value of r; then equation (17) gives you the value of L/m for which the free stone moves tangentially at this r. This equation is valid at all turning points and everywhere along a circular orbit.

We want to place the incoming spaceship into a circular orbit at $r = 20M$. But Section 18.4 tells us that there are *four* Types of circular orbits at every $r > r_{\text{ISCO}}$. Which of these four circular orbit Types do we choose for our incoming spaceship?

Choose Type 1 at $r = 20M$.

We choose the map energy of a stone to be positive, while map angular momentum can be either positive or negative. This limits circular orbits to either Type 1 or Type 4. Figure 4 in Section 18.4 shows the Type 1 circular orbit at $r = 4M$ to be stable; similarly for the Type 1 orbit at $r = 20M$. In contrast, the Type 4 circular orbit is unstable—too dangerous for our astronauts. Therefore we choose the Type 1 (stable) circular orbit.

Comment 3. Turning point symbols, a reminder

Figures in this chapter use *turning point* symbols from Definition 2 and Figure 1 in Section 18.3: The little open circle lies at the r-value of a *stable* circular orbit. The little filled circle lies at the r-value of an *unstable* circular orbit. The little half-filled circle lies at the r value of the half-stable innermost stable circular orbit, ISCO. Finally, the little filled diamond lies at a *bounce point*, where an incoming free stone "bounces" off the effective potential, reversing its r-component of motion.

Insertion orbit tangential at $r = 20M$.

We want the insertion orbit to be tangential at the instant when the unpowered spaceship reaches $r = 20M$. What map values E and L of the distant spaceship lead to its later tangential motion at $r = 20M$? We

TABLE 19.1 Numerical values at $r = 20M$ and $r = r_{\mathrm{ISCO}}$ for $a/M = (3/4)^{1/2}$

Values of	at $r = 20M$	at $r_{\mathrm{ISCO}} = 2.537\ 331\ 95M$
R^2	$400.825\ 000M^2$	$7.779\ 225\ 58M^2$
R	$20.020\ 614\ 4M$	$2.789\ 126\ 31M$
$2Ma/r$	$0.086\ 602\ 540\ 4M$	$0.682\ 626\ 807M$
$\omega = 2Ma/(rR^2)$	$2.160\ 607\ 26 \times 10^{-4}M^{-1}$	$0.087\ 749\ 969\ 5M^{-1}$
rH	$18.993\ 419\ 9M$	$1.453\ 750\ 16M$
rH/R	0.948 693 158	0.521 220 626
$1-(2M/r)$	0.9	0.211 770 458
$(L/m)_{\mathrm{insert}}$	$6.643\ 724\ 95M$	———
$(E/m)_{\mathrm{insert}}$	1.001	———
$v_{x,\mathrm{ring,insert}}$	0.314 955 478	———
$(L/m)_{\mathrm{Type\,1}}$	$4.712\ 495\ 61M$	$2.208\ 530\ 40M$
$(E/m)_{\mathrm{Type\,1}}$	0.975 638 130	0.858 636 605
$v_{x,\mathrm{ring,Type\,1}}$	0.229 120 545	0.620 784 509
$(L/m)_{\mathrm{transfer}}$	$2.678\ 687\ 02M$	$2.678\ 687\ 02M$
$(E/m)_{\mathrm{transfer}}$	0.957 725 762	0.957 725 762
$v_{x,\mathrm{ring,transfer}}$	0.132 614 709	0.692 683 307

arbitrarily choose incoming spaceship map energy $E/m = 1.001$, as we did in Section 9.2. With this choice, equation (17) yields the value of $(L/m)_{\mathrm{insert}}$ for the insertion orbit at $r = 20M$. Add this value to Table 19.1.

Subscripts in Table 19.1

DEFINITION 1. Subscripts in Table 19.1

Here are definitions of the subscripts in Table 19.1. All of them describe the motion of a free stone or an unpowered spaceship or probe.

insert: Quantities for a stone approaching from a great distance that leads it to move tangentially at the given r.

Type: Quantities for a stone in a circular orbit of that Type at the given r (Section 18.4).

transfer: Quantities for a stone in a transfer orbit between tangential motion at both of the given values of r.

ring: Value of the quantity measured in the local inertial ring frame at that r.

Comment 4. Significant digits

In this chapter we analyze several unstable (knife-edge) circular orbits. Interactive software such as GRorbits requires accurate inputs to display the orbit of an unpowered probe that stays in an unstable circular orbit for more than one revolution. To avoid clutter, we relegate to tables most numbers that have many significant digits.

Insert into circular orbit

The insertion maneuver shown in Figures 1 and 2 brings the unpowered spaceship to instantaneous tangential motion at $r = 20M$. Before it can move outward again, a tangential rocket thrust slows it down to the orbital speed of a stable Type 1 circular orbit at that r-value. What change in tangential velocity must this rocket thrust provide? To answer this question, we must choose a local inertial frame in which to measure tangential velocities. Sections 17.5 through 17.8 describe *four* different local inertial frames. Which one should we choose? Figure 5 in Section 17.5 shows that of our four local inertial frames, only the ring frame exists both outside the event horizon and inside the Cauchy horizon—locations where circular orbits also exist. Therefore we choose to measure the tangential velocity in the local ring frame.

The *ring frame* is the local rest frame of a ring rider who circles the black hole with map angular speed:

$$\frac{d\Phi}{dT} = \omega \equiv \frac{2Ma}{rR^2} \tag{18}$$

where Box 1 defines both ω and R^2. As with all local inertial frames, we define the ring frame so that local coordinate increments satisfy the flat spacetime metric,

$$\Delta\tau^2 \approx \Delta t_{\text{ring}}^2 - \Delta x_{\text{ring}}^2 - \Delta y_{\text{ring}}^2 \tag{19}$$

Doran metric

where each local coordinate difference equals a linear combination of global coordinate increments appearing in the global metric. The approximate Doran metric becomes:

$$\begin{aligned}\Delta\tau^2 \approx &\left(1 - \frac{2M}{\bar{r}}\right)\Delta T^2 - 2\left(\frac{2M\bar{r}}{\bar{r}^2 + a^2}\right)^{1/2}\Delta T\,\Delta r + \frac{4Ma}{\bar{r}}\Delta T\,\Delta\Phi \\ &- \frac{\bar{r}^2\,\Delta r^2}{\bar{r}^2 + a^2} + 2a\left(\frac{2M\bar{r}}{\bar{r}^2 + a^2}\right)^{1/2}\Delta r\,\Delta\Phi - \bar{R}^2\Delta\Phi^2 \ .\end{aligned} \tag{20}$$

Ring frame coordinates

We define ring frame coordinates by equations (77) to (80) of Section 17.8:

$$\Delta t_{\text{ring}} = \frac{\bar{r}H(\bar{r})}{R(\bar{r})}\Delta T - \frac{\beta(\bar{r})}{H(\bar{r})}\Delta r \tag{21}$$

$$\Delta y_{\text{ring}} = \frac{\Delta r}{H(\bar{r})} \tag{22}$$

$$\Delta x_{\text{ring}} = R(\bar{r})\left[\Delta\Phi - \omega(\bar{r})\Delta T\right] - \frac{\bar{r}\omega(\bar{r})}{\beta(\bar{r})}\Delta r \tag{23}$$

where Box 1 defines β. You can substitute equations (21) through (23) into (19) to verify that the result matches (20).

To complete the insertion of the incoming spaceship, we need to find the value of the rocket thrust required to put the ship into the Type 1 circular orbit at $r = 20M$. Appendix B has the general results. Here we use equation (94) for tangential motion.

$$v_{x,\text{ring}} = \frac{p_{x,\text{ring}}}{E_{\text{ring}}} = \frac{rH}{R^2}\left(\frac{L}{E - \omega L}\right) \tag{24}$$

TABLE 19.2 Rocket Thrusts in Instantaneous Initial Rest Frames (IIRF)

Thrust	at $r =$	$\Delta v_{x,\mathrm{IIRF}}$	Description	$m_{\mathrm{final}}/m_{\mathrm{initial}}$
#1	$20M$	$\Delta v_{x,\mathrm{IIRF1}} = -0.092\ 510\ 766\ 2$	into circular orbit	0.9113976
#2	$20M$	$\Delta v_{x,\mathrm{IIRF2}} = -0.099\ 530\ 031\ 6$	into transfer orbit	0.9049635
#3	$2.5373M$	$\Delta v_{x,\mathrm{IIRF3}} = -0.126\ 139\ 806$	into ISCO	0.8808964
#4	$2.5373M$	$\Delta v_{x,\mathrm{IIRF4}} = -0.545\ 847\ 072$	into transfer to r_1	0.5420231
#5	$2.5373M$	$\Delta v_{x,\mathrm{IIRF5}} = -0.402\ 281\ 976$	into transfer to r_2	0.4743450

NOTE: A first probe uses thrusts #2, #3, and #4 to carry it from the spaceship in orbit at $r = 20M$ to orbit r_1 inside the Cauchy horizon. A second probe uses thrusts #2, #3, and #5 to carry it from the spaceship to orbit r_2 inside the Cauchy horizon.

What insertion velocity change?

What "change in velocity" must the spaceship rocket thrust provide in order to convert its "insertion velocity" at $r = 20M$ to its "circular orbit velocity" at that r-value? Quotation marks in the preceding sentence warn us that values of *velocity* and *velocity change* depend on the local inertial frame from which we measure them. We measure velocities $v_{x,\mathrm{ring,insert}}$ and $v_{x,\mathrm{ring,Type\,1}}$ with respect to the local inertial ring frame. But what does the spaceship captain care about the ring frame? Indeed, from her point of view a stone at rest in the ring frame can be lethal! All she cares about are answers to questions like, "Do I have enough rocket fuel left to escape from this black hole?" The answer to this question depends only on the change in velocity in the spaceship's initial rest frame. In Chapter 9 we labeled the inertial frame in which the spaceship is initially at rest the **Instantaneous Initial Rest Frame (IIRF)** (Definition 2, Section 9.2). The present chapter describes five different IIRF velocity changes. Table 19.2 lists these velocity changes with the number 1 through 5 added to each subscript.

Instantaneous initial rest frame IIRF

A special relativity equation for addition of velocities—equation (54) of Section 1.13—allows us to use the two ring-frame velocities $v_{x,\mathrm{ring,Type\,1}}$ and $v_{x,\mathrm{ring,insert}}$ to calculate the required rocket-thrust velocity change $\Delta v_{x,\mathrm{IIRF1}}$:

$$\begin{aligned}\Delta v_{x,\mathrm{IIRF1}} &= \frac{v_{x,\mathrm{ring,Type\,1}} - v_{x,\mathrm{ring,insert}}}{1 - v_{x,\mathrm{ring,Type\,1}} v_{x,\mathrm{ring,insert}}} \qquad (25)\\ &= -0.092\ 510\ 766\ 2 \qquad \text{(place in circular orbit at } r = 20M)\end{aligned}$$

shown in Figure 2. Enter the numerical result in Table 19.2. This is the rocket-thrust velocity change ($-27\ 734$ kilometers/second) that places the incoming spaceship in the Type 1 circular orbit at $r = 20M$.

QUERY 1. Why use special relativity here?
Examine equation (25). Why do we assign the special relativity roles of v_{rel}, $v_{x,\mathrm{lab}}$, and $v_{x,\mathrm{rocket}}$ from equation (54) of Chapter 1 to $v_{x,\mathrm{ring,insert}}$, $v_{x,\mathrm{ring,Type1}}$, and $\Delta v_{x,\mathrm{IIRF1}}$ in equation (25)?

Every change in spaceship (or probe) velocity $\Delta v_{x,\mathrm{frame}}$ with respect to a local inertial frame requires a rocket burn. Every rocket burn uses fuel that

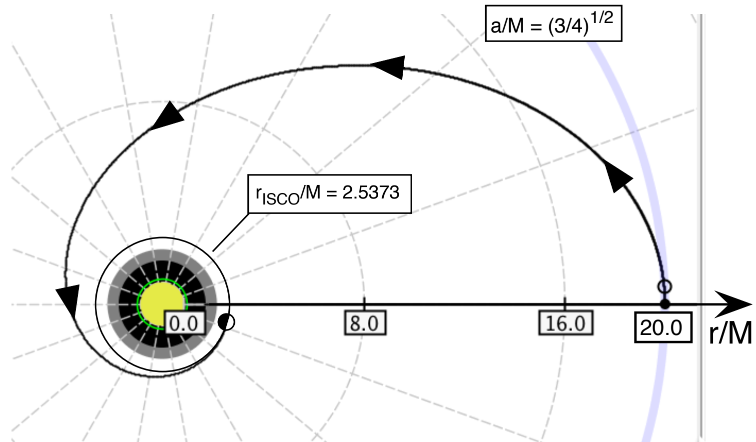

FIGURE 3 Transfer orbit in which the unpowered probe coasts from tangential motion at $r_{\rm A} = 20M$ to tangential motion at $r_{\rm B} = r_{\rm ISCO}$ and $\Phi_{\rm insert} = 350^{\rm o}$. Figure 4 indicates the required (single) tangential rocket thrust #2 to put the probe into this transfer orbit.

Use the photon rocket

changes the net mass of the spaceship or probe itself from initial mass $m_{\rm initial}$ to final mass $m_{\rm final}$. Query 2 recalls our analysis of the most efficient rocket, the so-called *photon rocket*, that combines matter and anti-matter and directs the resulting radiation out the back of the spaceship or probe. The final column of Table 19.2 lists the spaceship or probe mass ratio $m_{\rm final}/m_{\rm initial}$ for each burn described in that table.

QUERY 2. Mass ratios for transfer between circular orbits at $r = 20M$ and $r_{\rm ISCO}$.
Suppose our probe uses a photon rocket defined in Exercise 2 of Section 9.8, with the resulting mass ratio:

$$\frac{m_{\rm final}}{m_{\rm initial}} = \left[\gamma + \left(\gamma^2 - 1\right)^{1/2}\right]^{-1} \qquad \text{(photon rocket)} \qquad (26)$$

where $\gamma = [1 - (\Delta v_{x,\rm IIRF})^2]^{-1/2}$ with $\Delta v_{x,\rm IIRF}$ from the third column in Table 19.2. Verify all entries in the right hand column of Table 19.2.

19.3 ■ TRANSFER FROM THE INITIAL CIRCULAR ORBIT TO ISCO, THE INNERMOST STABLE CIRCULAR ORBIT

Balanced near the abyss

The spaceship completes observations in the stable Type 1 circular orbit at $r = 20M$. The captain wants to make further observations from a smaller circular orbit. To take the entire spaceship down to this smaller orbit requires a large amount of rocket fuel. Instead, the captain launches a small probe to the inner orbit to radio observations back to the mother ship.

Transfer to circular orbit at $r = r_{\rm ISCO}$.

What r-value shall we choose for the inner circular orbit? Be bold! Take the probe all the way down to the Innermost (prograde) Stable Circular Orbit at $r_{\rm ISCO} = 2.5373M$ for the black hole with $a/M = (3/4)^{1/2}$.

Comment 5. ISCO as a limiting case
The ISCO is hazardous because it's a "half stable" circular orbit that may lead to a death spiral inward through the event horizon. In practice the inner circular orbit r-value needs to be slightly greater than $r_{\rm ISCO}$ to make it fully stable. In what follows we ignore this necessary small r-adjustment.

Figures 3 and 4 illustrate the following two-step transfer process.

ORBIT TRANSFER STEPS

Step 1: A tangential rocket thrust

Step 2: A second tangential rocket thrust

Table 19.1 shows L and E values of our initial circular orbit at $r = 20M$. To carry out Step 1, we need to find two global quantities and one local quantity: map E and L of the transfer orbit plus rocket thrust #2 to put the probe at $r = 20M$ into this transfer orbit. Calculate the global quantities E and L first.

STEP 1A: CALCULATE $(E/m)_{\rm transfer}$ AND $(L/m)_{\rm transfer}$ OF THE TRANSFER ORBIT.

Transfer from $r = 20M$ to $r_{\rm ISCO}$

Call the outer r-value of the transfer orbit $r_{\rm A}$ for Above and the inner r-value $r_{\rm B}$ for Below. At these **turning points** $E = V_{\rm L}^{\pm}$. From equation (15) in Section 18.2 for $V_{\rm L}^{+}(r)$:

$$\left(\frac{E}{m}\right)_{\rm transfer} = \frac{V_{\rm L}^{+}(r_{\rm A})}{m} = \frac{V_{\rm L}^{+}(r_{\rm B})}{m} \qquad \text{(at turning points)} \qquad (27)$$

We use the $V_{\rm L}^{+}$ effective potential because the transfer orbit takes us from one Type 1 orbit at $r_{\rm A}$ to another Type 1 orbit at $r_{\rm B}$. Substitute for $V_{\rm L}^{+}$ from equation (16) in Section 18.2:

$$\left(\frac{E}{m}\right)_{\rm transfer} = \omega_{\rm A}\left(\frac{L}{m}\right)_{\rm transfer} + \frac{r_{\rm A}H_{\rm A}}{R_{\rm A}}\left[1 + \frac{1}{R_{\rm A}^2}\left(\frac{L}{m}\right)^2_{\rm transfer}\right]^{1/2} \qquad (28)$$

$$= \omega_{\rm B}\left(\frac{L}{m}\right)_{\rm transfer} + \frac{r_{\rm B}H_{\rm B}}{R_{\rm B}}\left[1 + \frac{1}{R_{\rm B}^2}\left(\frac{L}{m}\right)^2_{\rm transfer}\right]^{1/2} \qquad (29)$$

Our task is to find the value of $(L/m)_{\rm transfer}$ that makes the right side of (28) equal to the right side of (29). When this is accomplished, (28) yields the value of $(E/m)_{\rm transfer}$.

Find L/m of transfer orbit.

The Section 19.3 analysis for $r_{\rm A} = 20M$ gives us values of the coefficients on the right side of (28), already entered in the middle column of Table 19.1.

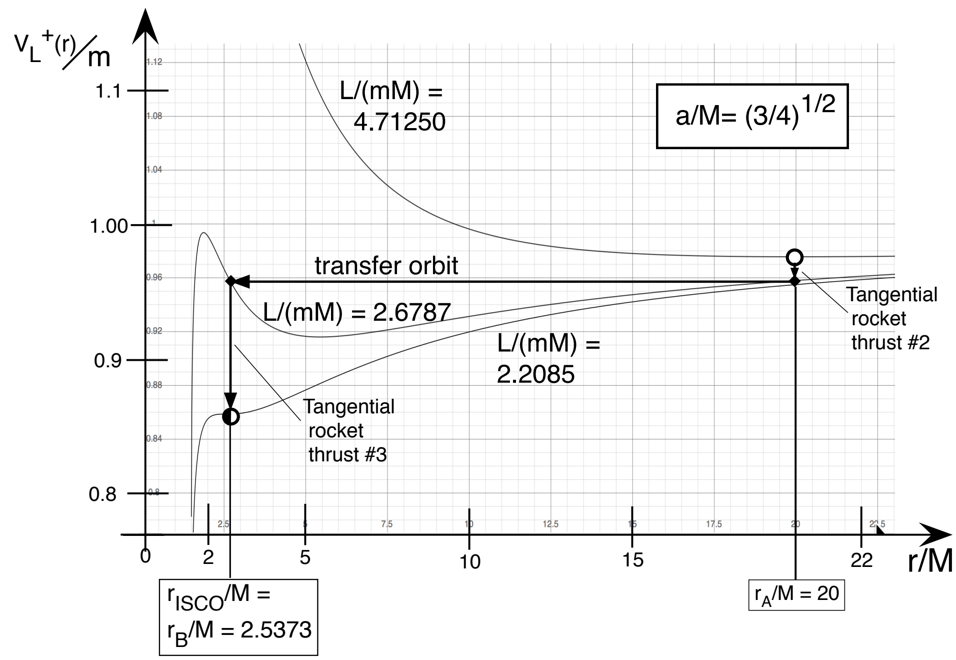

FIGURE 4 Rocket thrusts and resulting effective potential changes for transfer orbit between the stable Type 1 circular orbit at $r_{\mathrm{A}} = 20M$ and the half-stable Type 1 circular orbit at $r_{\mathrm{ISCO}} = r_{\mathrm{B}} = 2.5373M$ (Figure 3).

Now calculate coefficients on the right side of (29) using $r_{\mathrm{B}} = r_{\mathrm{ISCO}}$ and enter results in the right column of Table 19.1.

To find the value of $(L/m)_{\mathrm{transfer}}$, equate the right sides of (28) and (29). The result is a fourth order equation in $(L/m)_{\mathrm{transfer}}$, which has no straightforward algebraic solution. So we use a numerical software algorithm to find the value of $(L/m)_{\mathrm{transfer}}$ that makes equal the right sides of (28) and (29). Substitute the resulting value of $(L/m)_{\mathrm{transfer}}$ into equation (28) to find the value of $(E/m)_{\mathrm{transfer}}$ on the left side. Enter resulting values of $(L/m)_{\mathrm{transfer}}$ and $(E/m)_{\mathrm{transfer}}$ in the right-hand column of Table 19.1. Now use equation (94) to calculate values of $v_{x,\mathrm{ring,transfer}}$ at $r = 20M$ and at r_{ISCO}; enter them in Table 19.1.

STEP 1B: CALCULATE THE ROCKET THRUST VELOCITY CHANGE TO PUT THE PROBE INTO THE TRANSFER ORBIT.

IIRF2 transfer velocity change

What change in velocity must the rocket thrust provide to put the probe into the transfer orbit from $r = 20M$ to r_{ISCO}? This is our second tangential thrust to be given in an instantaneous initial rest frame IIRF, this time with the number 2 added to the subscript. From Table 19.1 and equation (54) of Section 1.13:

$$\Delta v_{x,\text{IIRF2}} = \frac{v_{x,\text{ring,transfer}} - v_{x,\text{ring,Type 1}}}{1 - v_{x,\text{ring,Type 1}} v_{x,\text{ring,transfer}}} \quad \text{(into transfer orbit . . .} \quad (30)$$
$$= -0.099\ 530\ 031\ 6 \qquad \text{from } r = 20M \text{ to } r_{\text{ISCO}})$$

shown as tangential rocket thrust #2 in Figure 4. Enter the numerical value in Table 19.2. This rocket thrust ring velocity change ($-29\ 838$ kilometers/second) inserts the probe from the circular orbit at $r = 20M$ into the transfer orbit that takes it down to instantaneous tangential motion at r_{ISCO}.

?

Objection 2. *In Figure 3 when the probe reaches the little half-black circle, will it automatically go into the circular orbit at r_{ISCO}?*

!

No, its map angular momentum is too high. Look at Figure 4. If there is no insertion rocket thrust, the probe will simply move back and forth along the "transfer orbit" line between r_{ISCO} and $r = 20M$. Step 2 describes the rocket-thrust insertion into ISCO.

STEP 2: ROCKET THRUST TO INSERT PROBE INTO ISCO

Insert into r_{ISCO} orbit.

The probe that follows the transfer orbit from $r = 20M$ arrives for an instant at global coordinates $r = r_{\text{ISCO}}$ and some value of Φ different from zero (Figure 3). At that instant it has tangential velocity $v_{x,\text{ring,transfer}}$ measured in local ring coordinates, which is too high for a circular orbit at r_{ISCO}. Equation (94) gives us this tangential ring velocity, calculated from selected values in the right column of Table 19.1. Enter the result in the lower right hand position in this table.

Now we want to change this tangential transfer velocity to the velocity $v_{x,\text{ring,Type 1}}$ of the circular orbit at r_{ISCO}. Use equation (94) and enter the result in Table 19.1.

IIRF3 insertion velocity change

Again we must calculate the change in velocity the rocket thrust must provide to put the probe into the circular orbit at r_{ISCO}. We measure this third tangential change—call it $\Delta v_{x,\text{IIRF3}}$ with the number 3 added to the subscript—with respect to the probe's instantaneous initial rest frame. From Table 19.1 and equation (54) of Section 1.13:

$$\Delta v_{x,\text{IIRF3}} = \frac{v_{x,\text{ring,Type 1}} - v_{x,\text{ring,transfer}}}{1 - v_{x,\text{ring,Type 1}} v_{x,\text{ring,transfer}}} \quad (31)$$
$$= -0.126\ 139\ 806 \qquad \text{(inserts into circular orbit at } r_{\text{ISCO}})$$

shown as tangential rocket thrust #3 in Figure 4. Enter the numerical result in Table 19.2. This velocity reduction ($-37\ 815$ kilometers/second) installs the probe into the Type 1 innermost stable circular orbit at r_{ISCO}.

Rocket mass ratios

Figure 4 shows that the transfer between $r = 20M$ and $r_{\text{ISCO}} = 2.5373M$ requires two rocket thrusts, #2 and #3, with values listed in Table 19.2, each with its mass ratio given in the last column of that table. Thrust #2 results in mass ratio $(m_{\text{final}}/m_{\text{initial}})_{\#2}$. The final probe mass of thrust #2 becomes the initial probe mass of thrust #3 in the mass ratio $(m_{\text{final}}/m_{\text{initial}})_{\#3}$. After both thrusts take place, the net result is that the probe arrives at r_{ISCO} with the net mass ratio equal to the product of the two mass ratios in the right hand column of Table 19.2:

$$\left(\frac{m_{\text{final}}}{m_{\text{initial}}}\right)_{\#2}\left(\frac{m_{\text{final}}}{m_{\text{initial}}}\right)_{\#3} = 0.9049635 \times 0.8808964 = 0.7971791 \qquad (32)$$

This completes our analysis of the transfer between the initial circular orbit at $r = 20M$ and the ISCO at $r_{\text{ISCO}} = 2.5373M$.

19.4 ■ ROCKET THRUSTS TO TRANSFER FROM ISCO TO CIRCULAR ORBITS INSIDE THE CAUCHY HORIZON

Teetering next to the singularity

Orbits inside the Cauchy horizon!

The probe carries out observations at r_{ISCO}. What's next? The captain examines two alternatives: observations from one of two *unstable* circular orbits inside the Cauchy horizon. We analyze both of theses alternatives.

?

Objection 3. *Either choice is stupid! Nothing comes back from inside the event horizon, not even a radio signal. So you cannot receive a report of what happens there. You are wasting resources to place the probe in any orbit inside the event horizon.*

!

Hamlet cautions us: "There are more things in heaven and earth, Horatio, than are dreamt of in your philosophy." Chapter 21 contains surprises about what rocket-blast maneuvers inside the event horizon can accomplish. In the meantime we can still predict what the diver inside the the Cauchy horizon experiences, as we did in Section 7.8 for the (doomed!) diver inside the event horizon of the non-spinning black hole, even though neither diver can report these observations to us on the outside.

This is the first of two sections on the probe transfer from the ISCO to orbits inside the Cauchy horizon. The present section derives rocket thrusts for transfers, summarized in Table 19.2. The following Section 19.5 plots the transfer orbits themselves. Why a separate section on these orbit plots? Because close to the singularity spacetime curvature is so large, and coordinates become so stretched, that plotting any orbit requires great care.

Start with a strategic overview: To install the probe into a *stable* circular orbit (Sections 19.2 and 19.3) requires a final rocket thrust to drop the probe's map energy into the minimum of the effective potential at that r (Figures 2 and 4). In contrast, we need no such final rocket thrust to install a probe into

No final insertion rocket thrust

TABLE 19.3 Circular orbits at r_{ISCO}, r_1, r_2 and some transfer orbits between them

Circular orbits	$r_{\text{ISCO}} =$ 2.537 331 95M Type 1 outside r_{EH}	$r_1 =$ 0.170 763 678M Type 1 inside r_{CH}	$r_2 =$ 0.353 627 974M Type 2 inside r_{CH}
L/m	2.208 530 40M	0.318 183 046M	0.849 088 850M
E/m	0.858 636 605	0.552 521 8506	0.619 345 540
R	2.789 126 311	3.092 447 193	2.262 034 177
ω	0.087 749 969 5 M^{-1}	1.060 621 78 M^{-1}	0.957 228 652 M^{-1}
rH/R^2	0.186 875 948M^{-1}	0.069 175 194 1M^{-1}	0.080 055 930 0M^{-1}
$v_{x,\text{ring,circle}}$	0.620 784 511	0.102 350 039	−0.351 423 150
Transfer orbits	From r_{ISCO}	to r_1	to r_2
L/m	—	0.318 183 046M	0.849 088 850M
E/m	—	0.552 521 851	0.619 345 540
$v_{x,\text{ring,transfer}}$	0.113 344 665	0.102 350 039	—
$v_{x,\text{ring,transfer}}$	0.291 232 033	—	−0.351 423 150

an *unstable* circular orbit such as those inside the Cauchy horizon. Why not? Because the transfer orbit is already at this maximum or minimum; the probe simply coasts onto that maximum or minimum (Figures 5 and 6). So we need only a single rocket thrust at r_{ISCO} to change map energy and map angular momentum to that of a circular orbit inside the Cauchy horizon. Now the details.

Transfer from r_{ISCO} to r_1

Transfer from r_{ISCO} to r_1: As a first alternative, transfer the probe from the r_{ISCO} orbit to the Type 1 unstable circular orbit at r_1 inside the Cauchy horizon (Figure 5). To do this, use a tangential rocket thrust that slows the probe so that it enters the transfer orbit in which it coasts directly into the unstable circular orbit at r_1.

Find L and E for transfer

How do we find values of L and E for this coasting orbit? Look again at equations (28) and (29). On the right side of (28), we know the value of r_{A} (the r-value of the ISCO), but we do not know the value of $(L/m)_{\text{transfer}}$. On the right side of (29), we do not know values of either r_{B} or $(L/m)_{\text{transfer}}$. Thus (29) has two unknowns, namely $(L/m)_{\text{transfer}}$ and $r_{\text{B}} = r_1$. However, we can find a second equation for these two unknowns, because we know that the circular orbit at r_{B} is Type 1, for which equation (31) in Section 18.4 takes the form

$$\left(\frac{L}{m}\right)_{\text{Type 1}} = \left(\frac{M}{r_{\text{B}}}\right)^{1/2} \frac{r_{\text{B}}^2 + a^2 - 2a(Mr_{\text{B}})^{1/2}}{\left[r_{\text{B}}^2 - 3Mr_{\text{B}} + 2a(Mr_{\text{B}})^{1/2}\right]^{1/2}} \quad \text{(circular orbit)} \quad (33)$$

Substitute this expression for (L/m) into equations (28) and (29), then equate the right sides of these two equations. The result is a (complicated!) equation

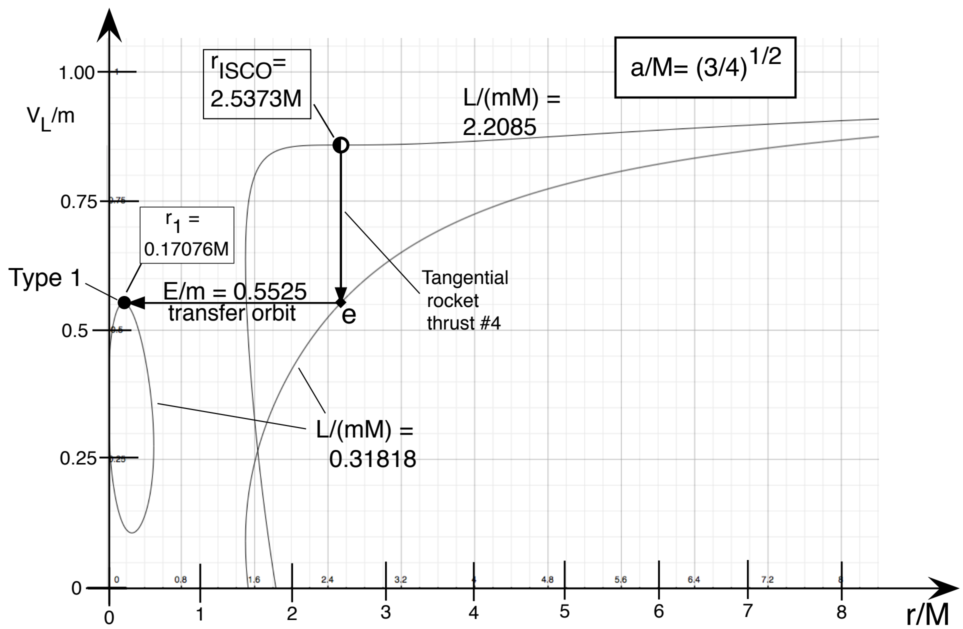

FIGURE 5 Tangential rocket thrust followed by coasting transfer orbit between ISCO (half-stable) prograde circular orbit and the Type 1 unstable circular at $r_1 = 0.17076M$, the *maximum* of the effective potential inside the Cauchy horizon.

in the single unknown r_{B}. Again use a numerical software algorithm to find the value of r_{B} and enter the result in the third column of Table 19.3.

QUERY 3. Identical table entries
Look at the two right-hand columns in Table 19.3, the ones labeled r_1 and r_2. Why are so many entries for circular orbits inside the Cauchy horizon the same as the corresponding entries for the transfer orbits?

Numerical values in Table 19.3 allow us to calculate the tangential $v_{x,\text{ring,transfer}}$ in (94) for the transfer orbit that starts at r_{ISCO} and ends at r_1 (Figure 5). The result is $v_{x,\text{ring,transfer}}$ =0.113 344 264 at r_{ISCO}, entered in Table 19.3.

IIRF4 transfer velocity change

Once again we must calculate the change in velocity the rocket thrust provides to put the probe into the transfer orbit at r_{ISCO}. Measure this change—call it $\Delta v_{x,\text{IIRF4}}$, with the number 4 added to the subscript—with respect to the instantaneous initial rest frame. From Tables 1 and 3 plus equation (54) of Section 1.13:

$$\begin{aligned}\Delta v_{x,\mathrm{IIRF4}} &= \frac{v_{x,\mathrm{ring,transfer}} - v_{x,\mathrm{ring,Type\,1}}}{1 - v_{x,\mathrm{ring,Type\,1}} v_{x,\mathrm{ring,transfer}}} \qquad \text{(into transfer orbit} \\ &= -0.545\ 847\ 072 \qquad\qquad \text{from } r_{\mathrm{ISCO}} \text{ to } r_1) \end{aligned} \tag{34}$$

shown in Figure 5. Enter the numerical value in Table 19.2. This change in rocket velocity (-163 641 kilometers/second) puts the probe into a transfer orbit between r_{ISCO} and r_1. Figure 5 shows that the probe then coasts into the unstable circular orbit at r_1 without the need for an insertion rocket thrust.

?

Objection 4. *Unbelievable! Are you really going to demand that a human-built rocket engine change the velocity of a probe by $\Delta v = 0.545\ 847$—more than half the speed of light? Get real!*

!

Even today we use multi-stage rockets to achieve large velocity changes. Still, mass ratios to achieve a speed reduction $c/2$—and even more the overall mass ratios in Items A and B of Query 4—require the resources of an **advanced civilization**, defined as one that can achieve any technical goal not forbidden by the laws of physics. Photon rocket technology may be in our future!

Transfer from r_{ISCO} to r_2

IIRF5 transfer velocity change

Transfer from r_{ISCO} to r_2: As a second alternative, the spaceship captain transfers the probe from the ISCO to the Type 2 unstable circular orbit at r_2, a minimum of the effective potential inside the Cauchy horizon. Figure 6 shows this maneuver. A tangential rocket thrust drops the map angular momentum of the probe to $L/m = 0.849\ 088\ 850M$. Then the probe coasts inward to the minimum of the effective potential at r_2 inside the Cauchy horizon, no insertion rocket thrust required.

The change in velocity the rocket thrust provides puts the probe into the transfer orbit at r_{ISCO}. We measure this change—call it $\Delta v_{x,\mathrm{IIRF5}}$, with the number 5 added to the subscript—with respect to the instantaneous initial rest frame. From Tables 1 and 3 plus equation (54) of Section 1.13:

$$\begin{aligned}\Delta v_{x,\mathrm{IIRF5}} &= \frac{v_{x,\mathrm{ring,transfer}} - v_{x,\mathrm{ring,Type\,1}}}{1 - v_{x,\mathrm{ring,Type\,1}} v_{x,\mathrm{ring,transfer}}} \qquad \text{(into transfer orbit} \\ &= -0.402\ 281\ 976 \qquad\qquad \text{from } r_{\mathrm{ISCO}} \text{ to } r_2) \end{aligned} \tag{35}$$

labeled "Tangential rocket thrust #5" in Figure 6. Enter the numerical result in Table 19.2. This change in velocity (-120 601 kilometers/second) puts the probe into a transfer orbit toward the unstable Type 2 circular orbit at r_2, shown in Figure 6. When the probe arrives there, it already has the map energy and map angular momentum of that unstable circular orbit, so does not require an insertion rocket thrust.

Recall our overall strategy: Thrust #1 takes the entire spaceship into the stable circular orbit at $r = 20M$. The spaceship then launches two separate

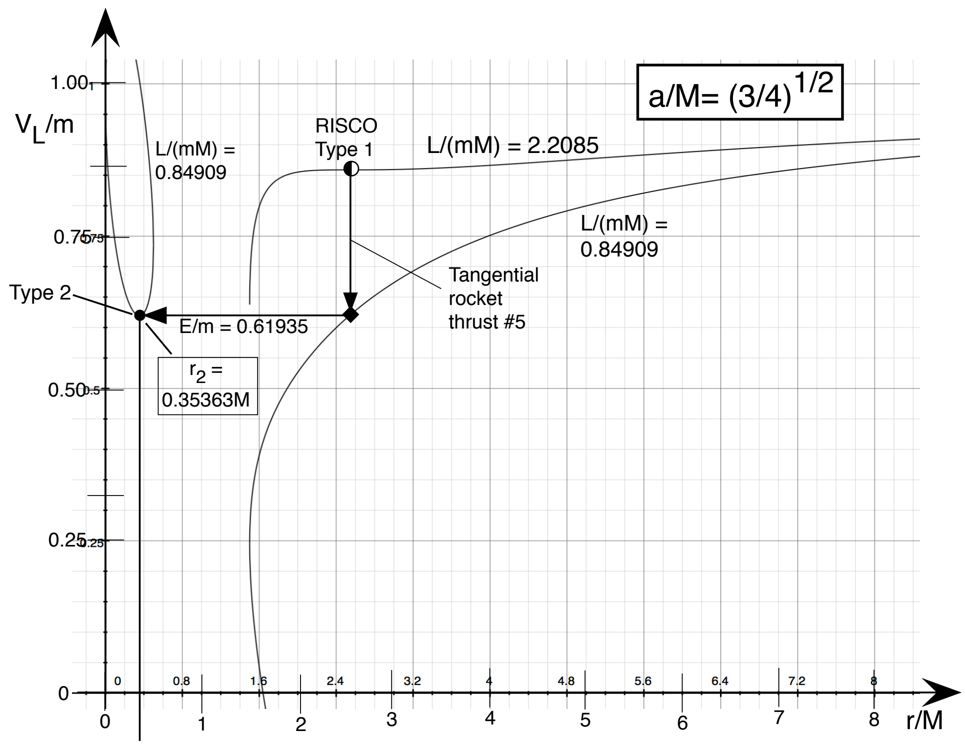

FIGURE 6 Transfer from Type 1 r_{ISCO} circular orbit to Type 2 unstable circular orbit at r_2, the *minimum* of the effective potential inside the Cauchy horizon.

probes. The first probe uses the sequence of thrusts #2, #3, and #4 to enter the unstable circular orbit at r_1 inside the Cauchy horizon. The second probe uses the sequence of thrusts #2, #3, and #5 to enter the unstable circular orbit at r_2 inside the Cauchy horizon.

QUERY 4. Net mass ratios for transfer between circular orbit r_{ISCO} and circular orbits inside the Cauchy horizon.

A. Analyze the entire sequence of thrusts #2, #3, and #4 that carry the first probe from the spaceship to the unstable circular orbit at r_1 inside the Cauchy horizon. What is the net mass ratio for this sequence of thrusts. [My answer: 0.4320895]

B. Next analyze the sequence of thrusts #2, #3, and #5 that carry the second probe from the spaceship to the unstable circular orbit at r_2 inside the Cauchy horizon. What is the net mass ratio for this sequence of thrusts. [My answer: 0.3781379].

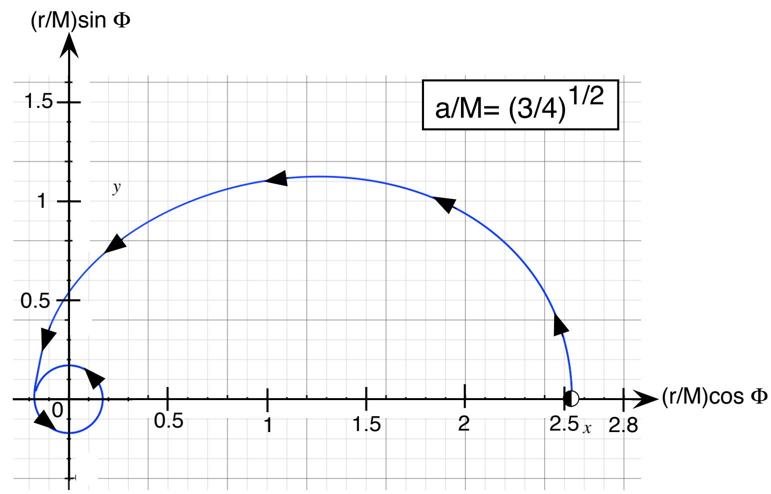

FIGURE 7 First plot of the transfer orbit between the circular ISCO and the circular orbit at $r_1 = 0.17076M$ inside the Cauchy horizon (Figure 5). This plot of $(r/M)\sin\Phi$ vs. $(r/M)\cos\Phi$ is the one we usually call an "orbit." This plot is totally correct, but near the singularity it misrepresents the geometry of spacetime.

19.5 ■ PLOTTING TRANSFER ORBITS FROM ISCO TO CIRCULAR ORBITS INSIDE THE CAUCHY HORIZON

One transfer, one failure

This section plots transfer orbits from the innermost stable circular orbit at $r_{\rm ISCO}$ to two different unstable circular orbits inside the Cauchy horizon: one at r_1, the maximum of an effective potential, the other at r_2, the minimum of another effective potential. For $a/M = (3/4)^{1/2}$, the circular orbit at $r_1 = 0.1707M$ lies very close to the singularity. Spacetime there is so radically warped that no global coordinate system—even Doran coordinates—gives us a picture that conforms to our everyday intuition. In what follows we do the best we can to find orbit plots that inform our intuition about this strange world.

TWO circular orbits inside the Cauchy horizon

Figure 7 shows a first orbit plot of the transfer from $r_{\rm ISCO}$ to r_1. This plot seems straightforward, with the singularity at $r \to 0$ as expected. But a closer look reveals that this first plot fails to correctly represent spacetime near the singularity.

To see this, look again at the Doran global metric, equation (4) in Section 17.2 when $dT = 0$, that is, on an $[r, \Phi]$ slice. Then the squared differential of measured distance $d\sigma^2$ expressed in Doran coordinates becomes:

$$\boxed{\begin{gathered} d\sigma^2 = \left[\left(\frac{r^2}{r^2+a^2}\right)^{1/2} dr - a\left(\frac{2M}{r}\right)^{1/2} d\Phi\right]^2 + \left(r^2+a^2\right) d\Phi^2 \qquad (36) \\ 0 < r < \infty, \quad 0 \le \Phi < 2\pi, \qquad dT = 0, \text{ on an } [r,\Phi] \text{ slice} \end{gathered}}$$

What happens to $d\sigma$—the differential of a measurable quantity—as $r \to 0$? The final $d\Phi^2$ term on the right side behaves reasonably; it goes to $a^2 d\Phi^2$ as $r \to 0$. In contrast, the first $d\Phi$ term blows up as $r \to 0$.

Singularity not a point.

However a little rearrangement simplifies this metric and allows us to predict a measurable result. Expand metric (36) and collect terms.

$$d\sigma^2 = \frac{r^2}{r^2+a^2}dr^2 - 2a\left(\frac{2Mr}{r^2+a^2}\right)^{1/2} dr d\Phi + \left(r^2 + a^2 + \frac{2Ma^2}{r}\right) d\Phi^2 \quad (37)$$

$$d\sigma^2 = \frac{r^2}{r^2+a^2}dr^2 - 2a\left(\frac{2Mr}{r^2+a^2}\right)^{1/2} dr d\Phi + R^2 d\Phi^2 \quad (38)$$

$$0 < r < \infty, \quad 0 \le \Phi < 2\pi, \qquad dT = 0, \text{ on an } [r,\Phi] \text{ slice}$$

The step between (37) and (38) applies the definition of R^2 in Box 1.

Now, let r become very small and see what the singularity looks like. The first two terms in global metrics (37) and (38) become negligibly small and the third terms become:

$$d\sigma^2 \to R^2 d\Phi^2 \to a^2\left(1 + \frac{2M}{r}\right) d\Phi^2 \qquad (r \ll a \le M) \quad (39)$$

Singularity has the topology of a circle.

As the value of r continues to decrease, the coefficient of $d\Phi^2$ *increases.* Two locations with the same small r-value but different Φ lie along a *circular* arc of length $R\Delta\Phi$. And σ, remember, is a measurable quantity. *The singularity of a spinning black hole has the topology of a circle, not a point!* In the limit of small r, we call the circular topology a **ring singularity.**

Now ask: Is there a way to plot transfer orbits so that the measurable result in (39) becomes apparent? Yes: Use R as the separation from the origin. Figure 8 shows such a plot. As we now expect from Figure 7, the probe starts moving inward but its trajectory soon deflects outward because R^2 increases as $r/(2M)$ decreases. R begins at $R = 2.7891M$ and ends at $R = 3.0924M$. Yet Figure 5 clearly shows that during this transfer the probe moves steadily inward from $r = 2.5373M$ to $r = 0.1708M$. A paradox!

To resolve this paradox, note that R is double-valued (Figure 1 in Section 17.2), and that as $r \to 0$, $R \to \infty$. *Conclusion:* Using R to plot the orbit creates a bigger problem than it solves.

Try plotting the same orbit in global map coordinates r and Φ, as in Figure 9. In this plot the global map angle Φ increases from zero at r_{ISCO} to a value that increases without limit at r_1 as the probe continues to circle there. This plot is correct but tells us nothing that we do not already know from Figure 7. And it is ugly!

New global coordinates: X and Y

So far we have failed to discover how to plot the transfer orbit between r_{ISCO} and r_1 in such a way that it correctly displays the singularity as a circle, while preserving inward motion. To accomplish this, we choose a new radial global coordinate that does not blow up as $r \to 0$, but correctly plots a circle there. This radial coordinate is $(r^2 + a^2)^{1/2}$, shown in Figure 10. The global Cartesian coordinates become:

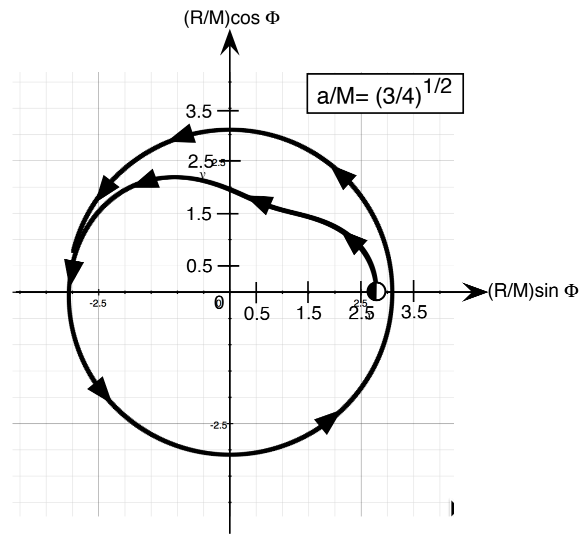

FIGURE 8 Second orbit plot of the transfer between ISCO and the circular orbit at $r_1 = 0.17076M$ inside the Cauchy horizon (Figure 5). This plot of $(R/M)\sin\Phi$ vs. $(R/M)\cos\Phi$ shows a strange coordinate behavior: The probe moves inward toward $r = 0$, yet arrives in a circular orbit of larger R than it started. See entries for R in Table 19.3.

$$X \equiv (r^2 + a^2)^{1/2} \cos\Phi \qquad \text{(global coordinates on } [r, \Phi] \text{ slice)} \qquad (40)$$

$$Y \equiv (r^2 + a^2)^{1/2} \sin\Phi \qquad (41)$$

$$X^2 + Y^2 > a^2, \quad 0 < r < \infty, \quad 0 \le \Phi < 2\pi \qquad (42)$$

Do global coordinates (40) and (41) correctly describe spacetime around a spinning black hole? They do, because they satisfy the conditions for a *good coordinate system* (Section 5.9). As we shall see, X and Y are good coordinates for much, but not all, of spacetime.

Figure 10 plots the transfer orbit in global X, Y coordinates.

GRorbits software uses $[X, Y]$ coordinates.

This book often employs the interactive software program GRorbits, which provides plots for many of our figures. Now it can be told: GRorbits makes its plots using X and Y coordinates.

?

Objection 5. *What's inside the blank disk at the center of Figure 10? The range of coordinates given in expressions (42) does not include the inside of this disk. Where can I find this inside region?*

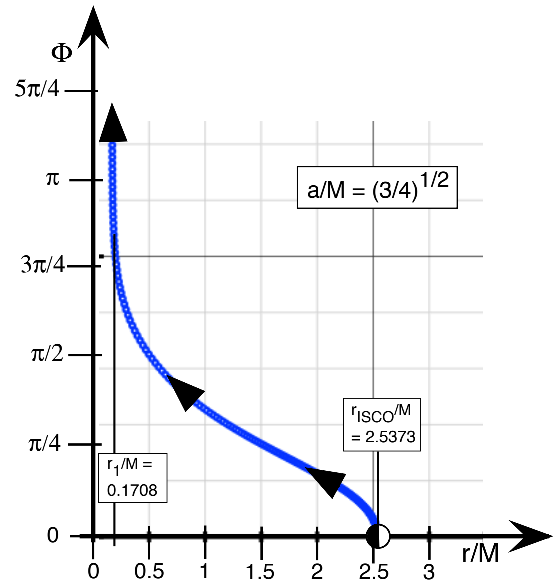

FIGURE 9 Second "orbit plot" of the transfer between ISCO and the circular orbit at $r_1 = 0.17076M$ inside the Cauchy horizon (Figure 5). This plot of Φ vs. r is not one we usually call an "orbit," but is perfectly valid as such.

!

There is no region inside the disk in the equatorial plane of the spinning black hole. Equations (40) through (42) show that points inside the ring at $r = 0$ have imaginary r-values, which is impossible.

Comment 6. Ring?
Except for gravitational waves (Chapter 16), almost all global metrics and global orbits in this book are restricted to the $[r, \Phi]$ slice. Therefore we can say nothing about the topology of any three-dimensional surface—perhaps a sphere or a cylinder—that might intersect the X, Y surface as our ring. However, advanced treatments show that the singularity of the Doran metric is confined to the $[r, \Phi]$ slice. It's a ring, not a sphere or cylinder. Moreover, we can access the central disk by traveling out of the equatorial plane to pass over or under the sigularity, as described in Chapter 21.

?

Objection 6. *The plot in which Figure: 7, 8, 9, or 10, is the correct one for the transfer orbit between circular orbits at $r_{\rm ISCO}$ and r_1?*

!

Every one of these orbits is equally valid and correct. Every one is distorted, because the geometry of spacetime near the spinning black hole is radically different from the flat space of our everyday lives. We select plots such as those in Figures 7 and 10 that display those features of the

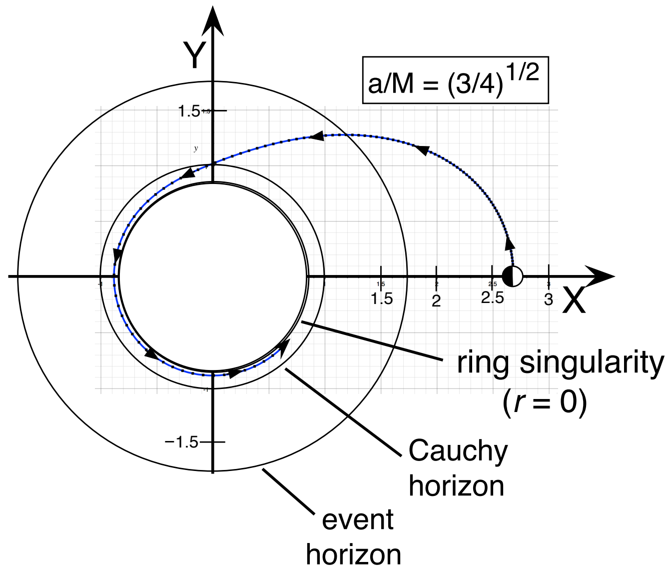

FIGURE 10 Fourth "orbit plot" of the transfer between ISCO and the circular orbit at $r_1 = 0.17076M$ inside the Cauchy horizon (Figure 5). This plot uses global coordinates X, Y.

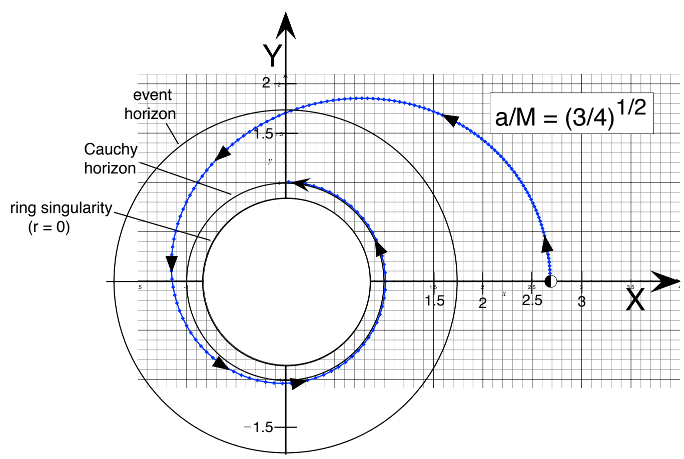

FIGURE 11 Unsuccessful attempt to plot the X, Y transfer orbit from $r_{\rm ISCO}$ to the minimum of the effective potential at $r_2 = 0.353\ 6M$ (Figure 6). The descending orbit shown here gets stuck at the Cauchy horizon and does not make it in to r_2. *Reason:* global Doran coordinates are not good everywhere. Chapter 21 presents new global coordinates that solve this problem.

geometry near a spinning black hole most likely to help us develop a useful intuition and ability to make predictions.

Hangup at the Cauchy horizon

So much for the transfer between $r_{\rm ISCO}$ to $r_2 = 0.17076M$. To complete our exploration inside the black hole, we also want to transfer from $r_{\rm ISCO}$ to $r_2 = 0.35363M$ at an effective potential minimum (Figure 6). This should be easier because $r_2 > r_1$ and spacetime is less warped at r_2, right? Figure 11 shows an attempt to make this plot. Oops! In this plot the probe does not move inward past the Cauchy horizon at $r_{\rm CH} = 0.5M$, shown in the figure at $X_{\rm CH} = (r_{\rm CH}^2 + a^2)^{1/2} = (1/4 + 3/4)^{1/2})M = M$.

Our history of *bad* global coordinates

Question: Why—in Figure 11—does the probe not pass inward through the Cauchy horizon? *Beginning of an answer:* We have run into this kind of problem before. Recall that the raindrop did not cross the event horizon of the non-spinning black hole when described in Schwarzschild global coordinates (Section 6.4). *Reason:* The Schwarzschild global t-coordinate is bad at the event horizon. *Solution:* Change to global rain coordinates (Section 7.5), whose T-coordinate ushers the raindrop inward through the event horizon to its doom. For the spinning black hole we started with Doran coordinates, chosen because they are good across the event horizon. But that is not enough to ensure that they are always good across the Cauchy horizon. What other coordinates are available?

Comment 7. Boyer-Lindquist t-coordinate bad at the event horizon
The exercises of Chapter 17 introduce the Boyer-Lindquist global coordinates for the spinning black hole, whose global metric is simpler than the Doran global metric. However, the Boyer-Lindquist t-coordinate is bad at the event horizon, where it increases without limit along the worldline of the raindrop.

Even Doran coordinates *bad.*

Doran global coordinates smoothly conduct our raindrop inward across the event horizon of the spinning black hole and all the way to the circular orbit at r_1, but fail to allow penetration of the Cauchy horizon on the way to the different circular orbit at r_2. Why are these two results different? Doran coordinates are okay for transfer to the circular orbit at r_1, but—it turns out—both T and Φ are bad at the Cauchy horizon for transfer to the circular orbit at r_2 (though they are good for transfer to r_1!). Figure 11 displays the problem with Φ: As $r \to r_{\rm CH}$, then $\Phi \to \infty$. To cross the Cauchy horizon we sometimes need different global coordinates. Chapter 21 explains why and shows us where new global coordinates can take us.

? **Objection 7.** *Is Nature fundamentally "bad"', or are you incompetent?*

! Nature is not bad. Mathematicians have proved that, for many curved spaces, it is impossible to cover the entire space with a single global coordinate system that is free of singularities. For these curved spaces there is no completely "good" coordinate system. The simplest example is a sphere: Earth's latitude and longitude coordinates are singular at the poles (Section 2.3), even though, for a non-spinning sphere, the poles are no different from any other points on the sphere. General relativity is difficult not because the mathematics is hard, but because we have to unlearn so many everyday assumptions that are false when applied to curved spacetime. One of these everyday false assumptions is the existence of a single global coordinate system that works everywhere.

Dispose of the probe.

To complete the Exploration Program for the Spinning Black Hole (Section 19.1), tip the probe off either unstable circular orbit inside the Cauchy horizon, so that it spirals into the singularity. Good job!

19.6 ■ ORBITING SUMMARY

Orbit descriptions

1. Effective potential plots (Figures 2, 4, 5, and 6) show us what orbits exist and help us to plot the transfer and circular orbits of an exploration program.
2. We must plot orbits using global coordinates, even though it is difficult to plot orbits in a way that is faithful to the twisted topology near the spinning black hole.
3. Sometimes one global coordinate system is not enough to cover the entire trajectory. It can take us only to the edge of a map; to go beyond that map, we need new global coordinates and a new map (Sections 2.5 and 7.5).
4. Doran global coordinates are effective across the event horizon but not necessarily through the Cauchy horizon. Also, Doran coordinates require help to show the topology of spacetime near the singularity, where a more revealing plot uses $(r^2 + a^2)^{1/2}$ rather than r or R.
5. *Preview:* Chapter 21 shows that the reason why Doran coordinates sometimes fail at the Cauchy horizon is that there are actually *two different* Cauchy horizons at the same $r_{\text{CH}} = M - (M^2 - a^2)^{1/2}$, called the *Cauchy horizon* and the *Cauchy anti-horizon.*

19.7 ■ THE PENROSE PROCESS MILKS ENERGY FROM THE SPINNING BLACK HOLE

Harness the black hole spin to hurl a stone outward.

The spinning black hole has an obvious motion that distinguishes it from the non-spinning black hole: *it spins!* Everywhere in physics, motion implies energy. Can we extract black hole spin energy for use? We know that an observer measures and extracts energy only in a local inertial frame. Can we find a local inertial frame in which the the black hole spin affects the measured energy of a stone, thus making it available for use? Roger Penrose found a way to harness the black hole spin as a local frame energy, then to send this energy to a distant observer. The present section examines what has come to be known as the **Penrose process**.

Three Penrose processes: energy conserved

Here are three physical processes in which energy does not appear to be conserved, but it is. We shall find that each process is an example of the Penrose process.

First process: A spaceship crosses inward through the static limit ($r_{\mathrm{S}} = 2M$) with map energy $E/m < 1$, a value less than the minimum escape energy $E/m = 1$. Even if its rockets are not powerful enough to increase E/m above the value one, a clever ejection of ballast allows it to escape.

Second process: A distant observer launches a stone toward a black hole. Over the course of a few weeks, the observer records outgoing photons followed by a high-speed outgoing stone. He measures the combined energy of the photons and outgoing stone to exceed that of the original stone.

Third process: A uranium atom with $E/m < 1$ radioactively decays while located between the static limit and the event horizon. A distant observer measures a thorium nucleus pass outward with greater total energy than the mass of the initial uranium atom.

In all three processes, an energetic body whizzes past a distant observer. To compensate for this emitted energy, the black hole swallows a second body (ballast, photons, or decay fragments) with map energy $E < 0$. In each of these Penrose processes the black hole mass decreases, along with its spin parameter a.

Third process: uranium nucleus decays

Begin with the third process, the spontaneous decay of a uranium nucleus into an alpha particle plus a thorium nucleus. Label this process as $b \rightarrow c + d$:

$$ {}^{235}\mathrm{U} \rightarrow {}^{4}\mathrm{He} + {}^{231}\mathrm{Th} \tag{43} $$

$$ b \rightarrow \quad c \quad + \quad d \qquad\qquad \text{(labels)} \tag{44} $$

Conservation of energy-momentum in ring frame

This reaction conserves the total energy and total momentum observed in every local inertial frame. We choose the ring frame. The ring frame observer verifies the following conservation statements:

$$ E_{\mathrm{ring},b} = E_{\mathrm{ring},c} + E_{\mathrm{ring},d} \tag{45} $$

$$ p_{x,\mathrm{ring},b} = p_{x,\mathrm{ring},c} + p_{x,\mathrm{ring},d} \tag{46} $$

$$ p_{y,\mathrm{ring},b} = p_{y,\mathrm{ring},c} + p_{y,\mathrm{ring},d} \tag{47} $$

We do not assume that the initial uranium nucleus (label b) is at rest in the ring frame; in general $E_{\mathrm{ring},b} > m_b$ with non-zero linear momentum components $p_{x,\mathrm{ring},b} = v_{x,\mathrm{ring},b}E_{\mathrm{ring},b}$ and $p_{y,\mathrm{ring},b} = v_{y,\mathrm{ring},b}E_{\mathrm{ring},b}$, and similar equations apply for each of the two daughter fragments.

Equations (45) through (47), combined with equations (96) and (97) in Appendix B imply that

$$ E_b = E_c + E_d \qquad\qquad \text{(map quantities)} \tag{48} $$

$$ L_b = L_c + L_d \tag{49} $$

Surprise conservation of map quantities

Surprise! Even though map energy and map angular momentum are not directly measured, they are conserved in the sense that when a uranium nucleus splits in two, the total map E and total map angular momentum L are each unchanged. This remarkable fact shows how map angular momentum and map energy can act as (conserved!) proxies for measurable quantities, as Section 18.7 anticipated.

More map energy out than in

To milk energy from the spinning black hole, a successful Penrose process requires that $E_\mathrm{d} > E_\mathrm{b}$; therefore $E_\mathrm{c} < 0$ in equation (48). We shall see that this is possible only for $r < r_\mathrm{S} = 2M$, and then only if $L_\mathrm{c} < 0$ (retrograde motion). Particle d recoils with increased map energy and map angular momentum: $E_d > E_b$ and $L_d > L_b$. This is surprising, because a spontaneous decay that takes place in the ring frame always *removes* energy:

$$E_d = E_b - E_c > E_b \tag{50}$$

$$E_{\mathrm{ring},d} = E_{\mathrm{ring},b} - E_{\mathrm{ring},c} < E_{\mathrm{ring},b} \tag{51}$$

The map energy increases while the ring frame energy decreases!

Difference milked from spin

The Penrose process takes advantage of the fact—shown in equation (91)—that ring frame energy is proportional to $E - \omega L$, not map energy E alone. Consequently, even if E increases, E_ring can decrease if L increases: $L_b - L_c = L_d$ must be sufficiently positive. The process works only if $\omega > 0$. Spacetime curvature "makes a contribution" to ring frame energy through the negative spin factor $-\omega$ in equation (91). When map angular momentum is also negative, $L < 0$, then spacetime curvature increases the ring frame energy: $E - \omega L > E$. The stone draws from spacetime curvature through the term $-\omega L$ to create a daughter nucleus (thorium) that escapes with more map energy than the initial nucleus (uranium) had when it arrived.

?

Objection 8. *How can a stone "draw from spacetime curvature" to increase its map energy? Never before have we equated curvature with energy.*

!

Curvature is *not* energy, just as map energy is not measured energy. Map energy depends on the metric, and therefore on spacetime curvature, even though measured energy is independent of the metric. Measurements are local, curvature is global. But global affects local!

Stone decays into light flash plus recoiling stone

Next look at the second process, in which a stone of mass m_b with (r, L_b, E_b) emits a light flash c with ring frame momentum components $(p_{x,\mathrm{ring},c}, p_{y,\mathrm{ring},c})$. The ring-frame energy of the light flash is $E_{\mathrm{ring,c}} = (p^2_{x,\mathrm{ring},c} + p^2_{y,\mathrm{ring},c})^{1/2}$. We want to find the mass, map angular momentum, and map energy of the stone—labeled d—that recoils from its backward emission of light. Note that $m_d < m_b$ because, in the rest frame of b, the light flash carries away energy. To determine the trajectory of stone d following the emission, we need both m_d and E_d because the motion depends on E_d/m_d and not on E_d alone.

Let $\phi_{\mathrm{ring},c}$ be the angle of photon momentum in the ring frame, defined so that

$$p_{x,\mathrm{ring},c} = E_{\mathrm{ring},c}\cos\phi_{\mathrm{ring},c} \qquad \text{(light)} \tag{52}$$

$$p_{y,\mathrm{ring},c} = E_{\mathrm{ring},c}\sin\phi_{\mathrm{ring},c} \qquad \text{(light)} \tag{53}$$

(For tangential retrograde motion, $\phi_{\mathrm{ring},c} = \pi$.) Equations (48), (96), and (97) lead to the following equations (54) and (55). Equation (56) for m_d derives from equations (52) through (55) when substituted into the special relativity equations $m_\mathrm{d}^2 = E_{\mathrm{ring},d}^2 - p_{\mathrm{ring},d}^2$ and $0 = E_{\mathrm{ring},c}^2 - p_{\mathrm{ring},c}^2$.

$$L_d = L_b - L_c = L_b - RE_{\mathrm{ring},c}\cos\phi_{\mathrm{ring},c} \tag{54}$$

$$E_d = E_b - E_c = E_b - E_{\mathrm{ring},c}\left(\frac{rH}{R} + \omega R\cos\phi_{\mathrm{ring},c}\right) \tag{55}$$

$$m_d = \left[m_b^2 + 2E_{\mathrm{ring},c}\left(-E_{\mathrm{ring},b} + p_{x,\mathrm{ring},b}\cos\phi_{\mathrm{ring},c} + p_{y,\mathrm{ring},b}\sin\phi_{\mathrm{ring},c}\right)\right]^{1/2} \tag{56}$$

Substitute equations (54) and (55) into equations (91) and (92) to give:

$$E_{\mathrm{ring},b} = \frac{R}{rH}(E_b - \omega L_b) \tag{57}$$

$$p_{x,\mathrm{ring},b} = \frac{L_b}{R} \tag{58}$$

$$p_{y,\mathrm{ring},b} = \pm\left(E_{\mathrm{ring},b}^2 - m_b^2 - p_{x,\mathrm{ring},b}^2\right)^{1/2} \tag{59}$$

We have written (L_d, E_d, m_d) in terms of $(r, m_b, L_b, E_b, E_{\mathrm{ring},c}, \phi_{\mathrm{ring},c})$ and can now determine under what conditions $E_\mathrm{d} > E_\mathrm{b}$.

Simplest case

The simplest case to analyze is for stone b to be in a tangential prograde circular orbit, $p_{x,\mathrm{ring},b} > 0$ and $p_{y,\mathrm{ring},b} = 0$. In this case, E_d is maximized and m_d is minimized when $\phi_{\mathrm{ring},c} = \pi$, that is when the light flash is emitted tangentially in the reverse (retrograde) direction.

?

Objection 9. *You said the stone was launched toward the black hole. That's not a circular orbit!*

!

The stone can be deflected into a circular orbit as it approaches the black hole, for example by encountering an accretion disk. The stone slowly loses energy to friction in the disk. After spiralling inward, it will be conveniently in a nearly circular prograde orbit inside the static limit from which the Penrose process can begin.

Fraction q of stone's mass becomes photon

We choose initial conditions $(r_b, L_b/m_b, E_b/m_b)$. The use of L_b/m_b and E_b/m_b as parameters instead of L_b and E_b generalizes the results to a stone of any mass m_b. All of the unknowns in equations (54) and (55) are now fixed except $E_{\mathrm{ring},c}/m_b$, which we rewrite for the case in which the fraction q of the mass m_b is emitted as a photon:

$$\frac{E_{\text{ring},c}}{m_b} = \frac{E_{\text{IIRF},c}}{m_b}\left(\frac{1-v_{x,\text{ring},b}}{1+v_{x,\text{ring},b}}\right)^{1/2} \equiv q\left(\frac{1-v_{x,\text{ring},b}}{1+v_{x,\text{ring},b}}\right)^{1/2} \tag{60}$$

where $E_{\text{IIRF},c}$ is the energy of photon c in the initial rest frame (the rest frame of b), and we have used the Doppler formula of special relativity, equation (48) in Section 1.13. The ratio q on the right side of (60) can also be expressed using (56) with $\phi_{\text{ring},c} = \pi$ in terms of the final/initial mass ratio of the stone:

$$\begin{aligned} m_d^2 &= m_b^2 - 2E_{\text{ring},c}\left(E_{\text{ring},b} + p_{x,\text{ring},b}\right) && (61)\\ 1-\frac{m_d^2}{m_b^2} &= 2\frac{E_{\text{ring},c}}{m_b}\frac{E_{\text{ring},b}}{m_b}\left(1+\frac{p_{x,\text{ring},b}}{E_{\text{ring},b}}\right) \\ \frac{1}{2}\left(1-\frac{m_d^2}{m_b^2}\right) &= \frac{E_{\text{ring},c}}{m_b}\frac{E_{\text{ring},b}}{m_b}\left(1+v_{x,\text{ring},b}\right) && (62)\end{aligned}$$

From special relativity:

$$\frac{E_{\text{ring},b}}{m_b} = \left(1-v^2_{\text{ring},b}\right)^{-1/2} = \left(1-v_{\text{ring},b}\right)^{-1/2}\left(1+v_{\text{ring},b}\right)^{-1/2} \tag{63}$$

Substitute from (63) with $v_{y,\text{ring},b} = 0$ into (62) and use (60):

$$\begin{aligned} \frac{1}{2}\left(1-\frac{m_d^2}{m_b^2}\right) &= \frac{E_{\text{ring},c}}{m_b}\left(\frac{1+v_{x,\text{ring},b}}{1-v_{x,\text{ring},b}}\right)^{1/2} && (64)\\ &= q\left(\frac{1-v_{x,\text{ring},b}}{1+v_{x,\text{ring},b}}\right)^{1/2}\left(\frac{1+v_{x,\text{ring},b}}{1-v_{x,\text{ring},b}}\right)^{1/2} = q \end{aligned}$$

so that finally the fraction q of stone b's mass that is carried away by photon c is given by the expression:

$$q \equiv \frac{E_{\text{IIRF},c}}{m_b} = \frac{1}{2}\left(1-\frac{m_d^2}{m_b^2}\right) \tag{65}$$

Assume that stone b is unable to escape the black hole without help, $E_b/m_b < 1$. This will be the case, for example, if the stone spirals inward in an accretion disk: the sequence of circular orbits in an accretion disk have $E/m < 1$ (Section 18.10). Can the stone escape by emitting a photon?

Answer this by evaluating E_d/m_d using (55) and (60):

$$\frac{m_d}{m_b}\left(\frac{E_d}{m_d}\right) = \frac{E_b}{m_b} - q\left(\frac{1-v_{x,\text{ring},b}}{1+v_{x,\text{ring},b}}\right)^{1/2}\left(\frac{rH}{R} - \omega R\right) \tag{66}$$

a similar calculation using (54) gives

$$\frac{m_d}{m_b}\left(\frac{L_d}{m_d}\right) = \frac{L_b}{m_b} + qR\left(\frac{1-v_{x,\text{ring},b}}{1+v_{x,\text{ring},b}}\right)^{1/2} \tag{67}$$

How large can E_d/m_d be? First, in order for the stone's map energy to increase, $E_d > E_b$, the final factor in (66) must be negative:

$$\omega R > \frac{rH}{R} \quad \text{(first condition for Penrose process)} \tag{68}$$

Definition of **ergoregion**

Equation (68) is equivalent to $r < r_\mathrm{S} \equiv 2M$. The region $r_\mathrm{EH} < r < r_\mathrm{S}$ is called the **ergoregion**.

QUERY 5. Where is a Penrose process possible?

A. Starting from (68), show that (70) implies $r < r_\mathrm{S} \equiv 2M$. This explains the origin of the term **ergoregion** for $r_\mathrm{EH} < r < r_\mathrm{S}$: inside the ergoregion it is possible to extract energy from a spinning black hole.

B. Show that for $r > r_\mathrm{S}$, all particles (both stones and photons) have $E > 0$. Thus, a stone with $E < 0$ is trapped inside the ergoregion. [Hint: use (97).]

C. Show that for $r < r_\mathrm{S}$, a retrograde photon ($\phi_\mathrm{ring} = \pi$) necessarily has $E < 0$, a prograde photon ($\phi_\mathrm{ring} = 0$) necessarily has $E > 0$, and a photon moving in other directions may have $E > 0$ or $E < 0$.

D. Show that as $r \to r_\mathrm{EH}$, a photon with even a slight backwards direction, $\phi_\mathrm{ring} = \frac{\pi}{2} + \epsilon$, has $E < 0$ and is therefore trapped.

Every Penrose process relies on the existence of particles with negative map energy. When is this possible? From (97), particle c (stone or photon) has negative map energy when

$$-v_{x,\mathrm{ring},c} > \frac{rH}{\omega R^2} \quad \text{(second condition for Penrose process)} \tag{69}$$

Conditions for the Penrose process

The two conditions can be combined into one equation:

$$\frac{rH}{\omega R^2} < -v_{x,\mathrm{ring},c} \leq 1 \quad \text{(Conditions for Penrose process)} \tag{70}$$

For a photon moving tangentially backward, $v_{x,\mathrm{ring},c} = -1$ so that

$$E_c = -E_{\mathrm{ring},c}\left(\omega R - \frac{rH}{R}\right) < 0 \quad (\text{for } r < r_\mathrm{S}) \tag{71}$$

The emission of a negative map energy photon inside the ergoregion increases the map energy of a stone but does not guarantee that the stone will escape, which requires $E_d/m_d > 1$. Equation (66) shows that this ratio depends on several quantities: the E/m of the original stone b, the velocity of the stone in the ring frame, and the ratio of final to original mass m_d/m_b or equivalently the fraction q of the stone's original mass that is converted to retrograde-moving photons. For a stone in a given orbit, q is the only quantity that we can vary. The Penrose process is most efficient when q is maximized.

Maximal energy: annihilation

Equation (65) shows that largest possible value is $q = \frac{1}{2}$. This limit corresponds to $m_d/m_b = 0$, i.e., the stone loses all its mass! If the stone is half matter and half anti-matter, their annihilation can extract the largest possible energy from the spinning black hole. Half the mass goes into the energy of a photon emitted in the prograde direction, and half to a photon emitted in the retrograde direction. The escaping photon ("stone d") has energy

$$E_d = E_b + \frac{1}{2} m_b \left(\frac{1 - v_{x,\mathrm{ring},b}}{1 + v_{x,\mathrm{ring},b}} \right)^{1/2} \left(\omega R - \frac{rH}{R} \right) \tag{72}$$

The energy extracted depends on the motion of the stone before it annihilates into photons. Amazingly, the map energy is largest when the stone is moving retrograde, $v_{x,\mathrm{ring},b} < 0$.

?

Objection 10. *This is crazy! How can going backwards increase the stone's map energy?*

!

You're right, this is wild, but it's true! As your intuition suggests, the map energy of stone b is *decreased* by backward motion, as shown by equation (97) with $v_{x,\mathrm{ring},b} < 0$. However, the stone's final map energy E_d also depends on the map energy of photon c. The measured energy of photon c depends on the motion of the emitter, stone b. From the Doppler formula (60), when $v_{x,\mathrm{ring},b}$ decreases, $E_{\mathrm{ring},c}$ increases and is positive: increasing stone b's velocity in the backward direction increases the energy of a photon emitted in that direction.

Now comes the real wildness: inside the ergoregion, the map energy E_c has the opposite sign to $E_{\mathrm{ring},c}$! Increasing $E_{\mathrm{ring},c}$ makes E_c more negative. The result? $E_d = E_b - E_c$ increases when $v_{x,\mathrm{ring},b}$ decreases.

Saving a crippled spaceship

Converting all one's mass to photons is a steep price to pay to escape from a black hole. Consider the first process described in the beginning of this section and ask what is the minimum energy fraction q that will allow a crippled spaceship to escape from inside the ergoregion without using rockets aside from a single thrust of a photon rocket. We seek the most frugal solution, which retains as much mass as possible.

Previous sections showed that it is very costly to transfer to circular orbits inside the Cauchy horizon (e.g., Table 19.2). Take instead the innermost stable circular orbit, the ISCO, to be the one from which we seek to return home. Taking advantage of the Penrose process requires $r_{\mathrm{ISCO}} < r_{\mathrm{S}}$. Exercise 1 below shows that this condition gives

$$\frac{a}{M} > \frac{2}{3}\sqrt{2} = 0.94281 \quad (r_{\mathrm{ISCO}} < r_{\mathrm{S}}) \tag{73}$$

We do not know whether real black holes have such high spins (though some astronomers think so, e.g. Risalti et al., Nature, 494, 449, 2013;

doi:10.1038/nature11938). (In 1974, Kip Thorne set a theoretical limit of $a/M < 0.998$: ApJ 191, 507, 1974).

Fast spinning black hole!

As an example, take $a/M = 0.96$, for which $r_{\rm EH} = 1.2M$. At the ISCO,

$$r_{\rm ISCO} = 1.84\ 300\ 573\,M\ , \quad \frac{L_b}{m_b} = 1.83\ 102\ 239\,M\ ,$$
$$\frac{E_b}{m_b} = 0.798\ 919\ 307\ , \quad v_{b,x,\rm ring} = 0.621\ 811\ 282\ . \tag{74}$$

QUERY 6. ISCO for a rapidly spinning black hole

Confirm the entries in equation (74) using equations (31), (32), and (75)–(77) of Chapter 18 and (94) below.

Given these parameters, find the minimum q for an escape orbit, by setting $E_d/m_d = 1$. Solve (66) using a numerical method and substitute into (67) to find

$$q = 0.173\ 658\ 866\ , \quad \frac{L_d}{m_d} = 2.50\ 581\ 328\,M\ . \tag{75}$$

After this photon rocket thrust, the spaceship has tangential velocity given by (24), which evaluates to

$$v_{x,{\rm ring},d} = 0.735\ 812\ 177 \tag{76}$$

As in previous sections, we calculate the velocity change provided by this rocket thrust to put the spaceship into an escape orbit from $r_{\rm ISCO}$. The velocity change in the instantaneous initial rest frame follows from equation (54) of Section 1.13:

$$\Delta v_{x,{\rm IIRF}b} = \frac{v_{x,{\rm ring},d} - v_{x,{\rm ring},b}}{1 - v_{x,{\rm ring},b}v_{x,{\rm ring},d}} \quad \text{(from the ISCO . . .} \tag{77}$$
$$= 0.210\ 153\ 964 \qquad \text{into an escape orbit)} \tag{78}$$

Compared with the velocity changes required to transfer from the ISCO to orbits inside the Cauchy horizon of a more slowly spinning black hole (Thrusts 4 and 5 in Table 19.2), this is economical!

Figure 12 shows the effective potentials of the spaceship (stone b) before and after the rocket thrust. Compare with thrust #3 in Figure 4, which inserted the spaceship into orbit at the ISCO. Figure 12 shows the opposite: ejection from the ISCO.

The final to initial mass ratio follows from equation (26) or (65):

$$\frac{m_d}{m_b} = (1-2q)^{1/2} = 0.807\ 887\ 533 \tag{79}$$

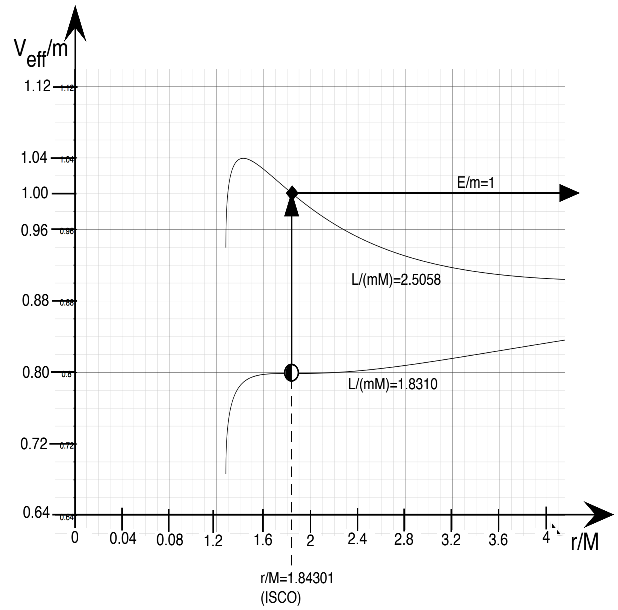

FIGURE 12 Effective potentials for a spinning black hole with $a/M = 0.96$ and two choices of the map angular momentum. The energy expended in the rocket thrust is less than the difference in map energy, providing a potential power source.

Extracting energy from the spinning black hole

This result seems almost mundane (it is comparable to thrust #3 in Table 19.2) until we compare it with E_b/m_b in equation (74), which is smaller than m_d/m_b. Although the difference is small, it reveals a crucial opportunity: the spinning black hole is an energy source!

To see this, recall that the map energy is the energy at infinity. As a stone spirals inward in an accretion disk, the photons emitted can escape to infinity, where their total energy is the difference in map energy, or $1 - (E_b/m_b) = 20.1\%$ of the original rest mass m_b. In principle, that energy is available to do work at infinity. Then, in order to escape back to infinity, a thrust must be applied that reduces m_b by a factor $1 - (m_d/m_b) = 19.2\%$. The energy difference is 0.9% of the rest mass, vastly more than the energy released by fission of uranium into thorium, and more even than is liberated by fusion of hydrogen into helium, 0.7%.

?

Objection 11. *Your numbers don't add up! You said that $q = 17.4\%$ of the initial mass goes into rocket thrust, and 80.8% is left. You're missing 1.8%!*

!

'The missing piece is the change in kinetic energy, $(\gamma - 1)m_d$, where γ is calculated using $\Delta v_{x,\mathrm{IIRF}b}$.

Justify claim: "Immense source of energy."

We can now justify the statement in Section 17.1, "The spinning black hole is an immense energy source, waiting to be tapped by an advanced civilization." Suppose you drop a stone from rest far from the black hole. Initially, $E/m = 1$ (a raindrop) and the stone enters an accretion disk. It looses map energy as it spirals inward (Section 18.8) emitting this map energy as photons. Recall that the energy of photons received at infinity is just the map energy lost, described in Sections 8.6 and 18.10 for accretion disks. By the time the stone reaches the ISCO, it has radiated a fraction $1 - E_b/m_b = 0.20108$ of its mass, as measured at infinity. In order to return to infinity, the stone's mass must decrease by a fraction $1 - m_d/m_b = 0.19211$. Thus the radiation received at infinity more than makes up for the loss of mass by the stone. We've extracted energy from the spinning black hole! This is possible because of the negative map energy of the retrograde photons emitted inside the static limit.

Comment 8. Many cycles; large extracted energy
The difference between E_b/m_b and m_d/m_b seems small, but a stone or spaceship can be reused to extract lots of energy over many cycles. Some of the energy radiated to infinity can be used to replenish the stone for another trip to the black hole. Note that the amount extracted is larger when the black hole spin is greater or the rocket thrust is applied closer to the event horizon.

?

Objection 12. *Great! We have an endless supply of energy; a perpetual motion machine! We just toss stones into the spinning black hole and program them to emit powerful laser pulses when they are inside the static limit.*

!

Sorry, this is a false hope. Here's the hitch: The photons with negative map energy fall into the black hole, where they decrease the black hole mass. We do not prove it here, but the gravitational effect of negative map energy is to decrease the gravitational field far from the black hole, exactly as if the black hole mass decreases. (Back to Newtonian physics for slow motion far from the black hole!) Still, the spinning black hole is a promising energy source for an advanced civilization.

Summary of the Penrose process for $a/M = 0.96$

Summary: Penrose process

1. Initially a stone with $E_b = m_b$ drops from rest at a great distance.
2. The stone enters an accretion disk, where it radiates 20.1% of its mass as it descends to the ISCO. The radiation—"quasar light"—travels to a great distance.
3. At the ISCO, the stone emits a photon rocket thrust; the surviving piece has mass $m_d = 0.808m_b$
4. The surviving piece with $E_d = m_d$ escapes to a great distance, where it comes to rest and can be furbished or replaced.
5. The stone's mass decreased by 19.2%, but more than this was received at a great distance as quasar light.

The Penrose process is reminiscent of Hawking radiation (Box 5 in Section 6.6), whereby energy is also extracted from a black hole. For Hawking radiation, however, the stone that falls into the black hole is a virtual stone, a temporary entity living on time borrowed from the Heisenberg Uncertainty Principle. In contrast the Penrose process photons with negative map energy are real, not virtual. In addition, non-spinning and spinning black holes both emit Hawking radiation, while the Penrose process works only for the spinning black hole.

Penrose process compared with Hawking radiation

19.8 ■ APPENDIX A: KILLER TIDES NEAR THE SPINNING BLACK HOLE

How close is a safe orbit?

In the Appendix of Chapter 9 we saw how local inertial frames are "spaghettified" by tidal accelerations when they move near a non-spinning black hole. Equations (38) to (40) and (46) to (48) in that chapter gave the expressions for the components of the tidal acceleration Δg_{local} for local inertial frames that move along the Schwarzschild r-direction and along the Schwarzschild ϕ-direction, respectively.

In the present Appendix A we list similar expression for the *spinning* black hole. We give all the equations in *Boyer-Lindquist coordinates.* (See the Project: Boyer-Lindquist Global Coordinates at the end of Chapter 17.) In the local inertial frames the $x-$, $y-$, and $z-$ directions are along the global $\phi-$direction, $r-$direction, and perpendicular to the spinning black hole's equator, respectively.

TIDES IN THE LOCAL RING FRAME

Expressions for the the tidal accelerations around the spinning black hole are messy. Fortunately, in the equatorial plane the equations reduce to a fairly simple form. For the local ring frame:

$$\Delta g_{\text{local,y}} \approx \frac{M}{\bar{r}^3}\frac{2+Z}{1-Z}\Delta y_{\text{local}} \tag{80}$$

$$\Delta g_{\text{local,x}} \approx -\frac{M}{\bar{r}^3}\Delta x_{\text{local}} \tag{81}$$

$$\Delta g_{\text{local,z}} \approx -\frac{M}{\bar{r}^3}\frac{1+2Z}{1-Z}\Delta z_{\text{local}} \tag{82}$$

where

$$Z \equiv \frac{a^2\bar{H}\bar{r}}{\left(\bar{r}^2+a^2\right)^2} \tag{83}$$

The value of the dimensionless quantity Z always lies between 0 and 0.043 (ref: Bardeen, Press, and Teukoilsky, 1972), so the deviations for the expressions from the Schwarzschild case are small.

As an exercise, check that for $a = 0$, the three equations above reduce to Schwarzschild expressions (38) through (40) in Chapter 9.

As another exercise, check that

$$\frac{\Delta g_{\text{local},x}}{\Delta x_{\text{local}}} + \frac{\Delta g_{\text{local},y}}{\Delta y_{\text{local}}} + \frac{\Delta g_{\text{local},z}}{\Delta z_{\text{local}}} \approx 0 \tag{84}$$

and compare the result with equation (45) in Chapter 9.

TIDES IN THE LOCAL ORBITER FRAME

The orbiter frame moves with speed v in the x-direction relative to the ring frame. The tidal acceleration components for the local orbiter frame are:

$$\Delta g_{\text{local,y}} \approx \frac{M}{\bar{r}^3}\frac{2+Z}{1-Z}\Delta y_{\text{local}} - 3\frac{M}{\bar{r}^3}\frac{\bar{H}a(\bar{r}^2+a^2)}{\bar{r}\bar{R}^2}\frac{v}{(1-v^2)^{1/2}}\Delta x_{\text{local}} \tag{85}$$

$$\begin{aligned} \Delta g_{\text{local,x}} \approx & -\frac{M}{\bar{r}^3(1-Z)}\left(1 - Z\frac{1+2v^2}{1-v^2}\right)\Delta x_{\text{local}} \\ & -3\frac{M}{\bar{r}^3}\frac{\bar{H}a(\bar{r}^2+a^2)}{\bar{r}\bar{R}^2}\frac{v}{(1-v^2)^{1/2}}\Delta y_{\text{local}} \end{aligned} \tag{86}$$

$$\Delta g_{\text{local,z}} \approx -\frac{M}{\bar{r}^3(1-Z)}\left(1 + Z\frac{2+v^2}{1-v^2}\right)\Delta z_{\text{local}} \tag{87}$$

Definition:
Shear terms

Note the second term on the right side of (85). It tells us that the y-component of the tidal acceleration depends on the x-coordinate too, not only the y-coordinate. Similarly, the second term on the right side of (86) tells us that the x-component of the tidal acceleration depends on the y-coordinate too, not only the x-coordinate. We call these two terms **shear** terms.

TIDES IN THE LOCAL RAIN FRAME

The tidal acceleration components in the local rain frame are:

$$\Delta g_{\text{local,y}} \approx \frac{M}{\bar{r}^3}\frac{2+Z}{1-Z}\Delta y_{\text{local}} - 3\frac{M}{\bar{r}^3}\frac{a(\bar{r}^2+a^2)^{3/2}}{\bar{r}^2\bar{R}^2}\frac{2M}{\bar{r}}\Delta x_{\text{local}} \tag{88}$$

$$\begin{aligned} \Delta g_{\text{local,x}} \approx & -\frac{M}{\bar{r}^3}\left(1 - \frac{3a^2(\bar{r}^2+a^2)}{\bar{r}^2\bar{R}^2}\left(\frac{2M}{\bar{r}}\right)^2\right)\Delta x_{\text{local}} \\ & -3\frac{M}{\bar{r}^3}\frac{a(\bar{r}^2+a^2)^{3/2}}{\bar{r}^2\bar{R}^2}\frac{2M}{\bar{r}}\Delta y_{\text{local}} \end{aligned} \tag{89}$$

$$\Delta g_{\text{local,z}} \approx -\frac{M}{\bar{r}^3}\left(1 + \frac{3a^2}{\bar{r}^2}\right)\Delta z_{\text{local}} \tag{90}$$

Again, note the presence of shear terms in the y-component and the x-component of the tidal acceleration: the second term on the right side of (88) and the second term on the right side of (89), respectively. A raindrop is not simply stretched in its local y-direction and compressed in its local x- and z-directions, but feels a sideways tension (shear) in its own rest frame too.

19.9 ■ APPENDIX B: RING FRAME ENERGY AND MOMENTUM

Measured energy and momentum

This appendix derives the map energy E and map angular momentum L of a stone from its ring frame energy $E_{\rm ring}$ and components of momentum $p_{x,\rm ring}$ and $p_{y,\rm ring}$ at a given r. The result is valid for any motion of the stone for which $H^2 > 0$, that is, everywhere except between the horizons. Start with equation (21):

$$\frac{E_{\rm ring}}{m} \equiv \lim_{\Delta\tau\to 0}\frac{\Delta t_{\rm ring}}{\Delta\tau} = \frac{rH}{R}\frac{dT}{d\tau} - \frac{\beta}{H}\frac{dr}{d\tau} = \frac{R}{rH}\left(\frac{E-\omega L}{m}\right) \tag{91}$$

The last step uses equation (111) of Section 17.10. Next, apply similar limits to equations (22) and (23) to obtain momentum components in the local ring frame:

$$\frac{p_{x,\rm ring}}{m} \equiv \lim_{\Delta\tau\to 0}\frac{\Delta x_{\rm ring}}{\Delta\tau} = R\left(\frac{d\Phi}{d\tau} - \omega\frac{dT}{d\tau}\right) - \frac{r\omega}{\beta}\frac{dr}{d\tau} = \frac{L}{mR} \tag{92}$$

$$\frac{p_{y,\rm ring}}{m} \equiv \lim_{\Delta\tau\to 0}\frac{\Delta y_{\rm ring}}{\Delta\tau} = \frac{1}{H}\frac{dr}{d\tau} \tag{93}$$

The velocity components in the local ring frame follow from these equations:

$$v_{x,\rm ring} = \frac{p_{x,\rm ring}}{E_{\rm ring}} = \frac{rH}{R^2}\left(\frac{L}{E-\omega L}\right) \tag{94}$$

$$v_{y,\rm ring} = \frac{p_{y,\rm ring}}{E_{\rm ring}} = \frac{r}{R}\left(\frac{m}{E-\omega L}\right)\frac{dr}{d\tau} \tag{95}$$

Expressions for map L and E.

Solve equations (91) and (92) for the map constants of motion in terms of the locally-measured ring energy and ring x-momentum:

$$L = Rp_{x,\rm ring} \qquad \text{(not between horizons)} \tag{96}$$

$$E = \left(\frac{rH}{R}\right)E_{\rm ring} + \omega R p_{x,\rm ring} = E_{\rm ring}\left(\frac{rH}{R} + \omega R v_{x,\rm ring}\right) \tag{97}$$

Section 19.7 uses these two equations in the description of the Penrose process.

19.10 ■ EXERCISES

1. When the ISCO lies at the static limit

The innermost stable circular orbit (ISCO) for the non-spinning black hole lies at $r = 6M$. For the non-spinning black hole there is no distinction between prograde and retrograde orbits. For the maximum spinning black hole ($a/M = 1$), the prograde ISCO drops to $r_{\rm ISCO1} = M$, while the retrograde orbit rises to $r_{\rm ISCO2} = 9M$. Figure 15 in Section 18.9 plots $r_{\rm ISCO}$ as a function of a/M for both prograde and retrograde circular orbits.

A. What is the intermediate value of a/M at which the prograde ISCO lies at the same r-value as the static limit, $r_{\rm S} = 2$? Use equations (75)—(77) of Section 18.8 to show that this intermediate value is $a/M = 0.94281$.

B. Verify that the numerical value of a/M in Item A is equal to $2^{3/2}/3$.

C. What is the r value of the retrograde ISCO for the value of a/M in Item A?

2. Choose incoming spaceship energy E/m for exploration program

Figure 2 shows that our explorers choose $E/m = 1.001$ for their initial energy as they start their journey from far away towards the spinning black hole. Justify this choice for the incoming value of E/m. Why should they not choose a value of E/m much larger than this? a value of E/m much closer to 1 than this? Are your reasons fundamental to general relativity theory or practical for particular spaceships and black holes?

3. Can a transfer orbit violate Kepler's second law?

Examine the second-to-last row of Table 19.3. For the transfer orbit between the circular orbit at $r_{\rm ISCO} \approx 2.537M$ and the circular orbit at $r_1 \approx 0.170M$, the value of $v_{x,\rm ring,transfer}$ appears to contradict Kepler's second law: The freely-moving probe appears to move faster at the larger r-coordinate than at the smaller r-coordinate. Explain how this is possible.

4. What kind of motion is raindrop motion?

Section 19.1 reviewed definitions of prograde/retrograde motions and forward/backward motions. Does *raindrop* motion provide the dividing line between forward and backward motion? between prograde and retrograde motion? Summarize your answers in a clear definition of *raindrop motion.*

5. "Size" of the ring singularity

How large is the ring singularity at r = 0?

A. Is the size of the ring singularity zero, as Figure 7 in Section 19.5 seems to show?

B. Does the *radial* size of the ring singularity equal the value of the spin-parameter a, as Figure 10 and equation (42) seem to imply?

C. Is the the ring singularity infinitely large, as Figure 8 and equation (39) seem to say? Show that from equation (39):

$$\text{circumference} = \lim_{r\to 0} 2\pi R = \lim_{r\to 0} 2\pi a \left(1 + \frac{2M}{r}\right)^{1/2} = \infty \qquad (98)$$

D. If the ring singularity is indeed infinitely large, as Item C implies, does this mean that the ring singularity extends to infinity and embraces the entire Universe? If so, why the limit $r \to 0$ in equation (98)?

E. From results of Items A through D, explain why quotes embrace the word "Size" in the title of this exercise.

6. Spacetime trajectory or spatial trajectory of the transfer orbit?

Figures 7, 9 and 10 are distorted maps, visual representations of transfer orbit, similar to the way that every flat map necessarily gives a distorted view of an arbitrary airplane route on Earth's spherical surface. But do these at least correctly depict the *spatial* trajectory of the transfer orbit? To answer this question look at the coordinates on the axes of these figures to check whether those coordinates are spacelike or timelike.

19.11 ■ REFERENCES

The original reference for the Penrose process is R. Penrose and R. M. Floyd, "Extraction of Rotational Energy from a Black Hole," Nature Physical Science. Volume 229, pages 177-179 (1971).

J. M. Bardeen, W. H. Press, and S. A. Teukolsky, "Rotating Black Holes: Locally Nonrotating Frames, Energy Extraction, and Scalar Synchrotron Radiation," The Astrophysical Journal, Volume 178, pages 347-369 (1972)

Download file name: Ch19OrbitingSpinningBH17115v2.pdf